BNL-222938-2022-JAAM

Stomatal conductance, not biochemistry, drives low temperature acclimation of photosynthesis in Populus balsamifera regardless of nitrogen availability

R. Kong, D. Way

To be published in "Plant Biology"

April 2022

Environmental and Climate Sciences Department

Brookhaven National Laboratory

U.S. Department of Energy

BNL Program Development

DISCLAIMER

Stomatal conductance, not biochemistry, drives low temperature acclimation of photosynthesis in *Populus balsamifera* regardless of nitrogen availability

Ricky S. Kong[1*], Danielle A. Way[1,2,3], Hugh A.L. Henry[1], Nicholas G. Smith[4]

[1] The University of Western Ontario, Department of Biology, London, ON, N6A 5B7, Canada
[2] Duke University, Nicholas School of the Environment, Durham, NC, 27710, USA
[3] Brookhaven National Laboratory, Environmental and Climate Sciences Department, Upton, NY, 11973, USA
[4] Texas Tech University, Department of Biological Sciences, Lubbock, TX, USA

Email: *rkong9@uwo.ca
Phone: +519 661-2111 x 81548
Address: 1151 Richmond Street, London, Ontario, Canada, N6A 5B7

ABSTRACT

Low temperature thermal acclimation may require adjustments to nitrogen and water use to sustain photosynthesis due to slow enzyme functioning and high-water viscosity. However, understanding of photosynthetic acclimation to temperatures below 11 °C is limited. We acclimated *Populus balsamifera* to 6 and 10 °C (6A and 10A, respectively) and provided the trees with either high or low N fertilizer. We measured net CO_2 assimilation rates (A_{net}), stomatal conductance (g_s), maximum rates of Rubisco carboxylation (V_{cmax}) and electron transport (J_{max}), and dark respiration (R_d) at leaf temperatures of 2, 6, 10, 14 and 18 °C, along with leaf N concentrations. The 10A trees had higher A_{net} than the 6A trees at warmer leaf temperatures, which was correlated with higher g_s in the 10A trees. The instantaneous temperature responses of V_{cmax}, J_{max} and R_d were similar for trees from both acclimation temperatures. While soil N availability increased leaf N concentrations, this had no effect on acclimation of photosynthesis or respiration. Our results indicate that acclimation below 11 °C occurred primarily through changes in stomatal conductance, not photosynthetic biochemistry, and was unaffected by short-term N supply. Thermal acclimation of stomatal conductance should therefore be a priority for future carbon cycle model development.

ADDITIONAL KEYWORDS

Balsam poplar, Chilling, Cold acclimation, Fertilization, Photosynthetic capacity, Respiration, Thermal acclimation

INTRODUCTION

Photosynthesis, which represents the largest flux of C between the atmosphere and the Earth's surface (Ciais *et al.* 2013), will be impacted by future changes in global mean temperature (Beer *et al.* 2010). In response to sustained changes in temperature, thermal acclimation of photosynthesis can occur; this results in a change in short-term photosynthetic responses to temperature in leaves acclimated to different temperatures (Way and Yamori 2013). Thermal acclimation can result from changes in membrane fluidity and the synthesis of stress-related proteins that alter the photosynthetic thermal optimum (Hikosaka *et al.* 2006) or changes in the allocation of resources to carboxylation and photosynthetic electron transport that alter the capacity for CO_2 fixation (Way and Sage 2008). These adjustments can occur within days of exposure to new temperature conditions (Campbell *et al.* 2007; Smith and Dukes 2017) and may help offset reductions in photosynthesis that would otherwise result from the change in temperature (Way and Sage 2008; Mathur *et al.* 2014; Rogers *et al.* 2017*a*; Dusenge *et al.* 2019).

Photosynthesis is an important component of the terrestrial biosphere models (TBMs) that are used to predict how CO_2 fluxes between the atmosphere and the land surface will respond to different future climate scenarios (Rogers *et al.* 2017*a*). However, these models typically do not consider thermal acclimation of photosynthesis (Smith and Dukes 2013). TBMs that have incorporated photosynthetic thermal acclimation have found that C uptake is significantly increased compared to models that do not incorporate acclimation (Lombardozzi *et al.* 2015; Smith *et al.* 2016; Mercado *et al*. 2018), which can alter our predictions of future climate change (Smith *et al*. 2017).

The Kattge and Knorr (2007) model (hereafter referred to as KK 2007) is the most commonly used model for photosynthetic temperature acclimation in TBMs, and the functions in this model can improve TBM carbon cycle predictions (Smith *et al.* 2016). The KK 2007 model predicts increases in the thermal optima of the instantaneous temperature responses of both the maximum rates of ribulose-1,5-bisphosphate carboxylase/oxygenase (Rubisco) carboxylation (V_{cmax}) and photosynthetic electron transport (J_{max}) with increasing acclimation temperature (Kattge and Knorr 2007). The KK 2007 model also predicts an increase in investment in V_{cmax} relative to J_{max} at increased acclimation temperatures. The KK 2007 model has been parameterized with species acclimated to temperatures from 11–35 °C and produces output consistent with data from controlled environment studies conducted across this same temperature

range (Smith and Dukes 2017, Scafaro *et al.* 2017). However, due to the lack of data that address acclimation to temperatures below 11 °C, TBMs are forced to either extrapolate the acclimation response to temperatures outside of the KK 2007 dataset or they do not include acclimation temperatures below 11 °C. Recent work has highlighted the danger of extrapolating these types of equations outside of the temperature ranges for which they were developed (Stinziano *et al.* 2019), emphasizing the need for measurements of V_{cmax} and J_{max} at low leaf temperatures and in trees acclimated to low temperatures. While recent work has extended the formulations of the KK 2007 model to lower temperatures using an observational dataset (Kumarathunge *et al.* 2019), these responses have gone untested in controlled experiments.

Results from Rogers *et al*. (2017*b*) suggest that trees acclimated to low temperatures may require high leaf nitrogen (N_{leaf}) to sustain high basal rates of V_{cmax} and J_{max}, given that N is required to build the enzymes that support these photosynthetic processes (Evans and Seemann 1989; Walker *et al.* 2014). This suggestion is consistent with environmental gradient studies and data from high latitudes, which have demonstrated greater N investment in V_{cmax} and J_{max} in colder regions (Ali *et al.* 2015, Smith and Dukes 2018). Thus, soil N availability may dictate the degree to which trees can satisfy high N demands at low temperatures (Yamori *et al.* 2014) and the degree to which they can thermally acclimate photosynthesis. Although plant N availability is limited in many terrestrial ecosystems, N inputs from atmospheric N deposition and intensive agriculture (Vitousek *et al.* 1997; Galloway *et al.* 2004) may allow trees a greater capacity to adjust their photosynthetic rates by providing the N required to synthesize increased concentrations of photosynthetic enzymes (Nunes *et al.* 1993). Nonetheless, while Rogers *et al*. (2017*b*) found photosynthetic capacity was dependent on N levels, they did not examine changes in the thermal sensitivity of photosynthetic capacity resulting from acclimation, which limits our understanding of the mechanisms driving acclimation and the ability for these responses to be included in TBMs.

Photosynthetic temperature acclimation may also be impacted by water availability (Lin *et al.* 2012; Reich *et al.* 2018, Kumarathunge *et al.* 2020). Water limitations may be particularly important at low temperatures, where high viscosity of water can lead to more costly water movement (Roderick and Berry 2001; Franks and Brodribb 2005). As a result, plants may acclimate by reducing stomatal conductance at low temperatures (Prentice *et al.* 2014), thus

limiting photosynthesis if biochemical capacity (V_{cmax} and J_{max}) is not increased to match the reduction in CO_2 supply.

Similar to photosynthesis, leaf respiration can acclimate to elevated temperatures, which also dramatically impacts the results from TBM simulations (Atkin *et al.* 2008). However, the mechanisms underlying thermal acclimation of respiration remain unclear (Dusenge *et al.* 2019). Acclimation of respiration has been observed across many different species, where respiration rates are reduced for the trees acclimated to higher temperatures, relative to control trees at a common measurement temperature (Slot and Kitajima 2015). These results have also been confirmed across environmental gradients (Smith and Dukes 2018). Acclimation of respiration to low temperatures may also depend on soil N availability, because higher respiration rates at these low temperatures may require higher quantities of respiratory enzymes.

We examined low temperature acclimation in *Populus balsamifera* (balsam poplar), a widespread and high N-demanding tree species (Chapin III 1996; Soolanayakanahally *et al.* 2013), under two different soil N concentrations. This species can be found throughout most of Canada, and its distribution in North America extends north to Alaska and south towards Colorado (Peterson and Peterson, 1992). Balsam poplar is a lowland species common to riparian sites that are rich with nutrients (Peterson and Peterson 1992; Rogers *et al*. 2020). *Populus* trees exhibit thermal acclimation of carbon assimilation when grown at high temperatures (Benomar *et al.* 2019), but little is known about their response to low temperatures.

In this study, following initial growth at 10 °C, we acclimated half of the study trees to 6 °C for six days and compared the thermal sensitivity of gas exchange to those trees maintained at 10 °C (i.e. the trees kept at 10 °C served as controls). We hypothesized that thermal acclimation to 6 °C would result in higher A_{net} at low leaf temperatures (< 6 °C) compared to the 10 °C control trees, but would reduce A_{net} at higher leaf temperatures (> 10 °C). We expected this to coincide with increased V_{cmax}, J_{max} and R_d in low temperature-acclimated trees. Because leaves require N to build enzymes, we hypothesized that high N fertilizer applied during the acclimation period would improve low temperature acclimation. Specifically, we predicted that thermal acclimation would be constrained under low soil N, and we therefore expected lower A_{net}, V_{cmax} J_{max}, and R_d in low N trees relative to high N trees acclimated to low temperatures.

METHODS AND MATERIALS

Plant establishment

Dormant, one-year old balsam poplar trees (saplings) with fully developed buds were purchased from St. Williams Nursery in Norfolk, ON, Canada. The trees originated from Seed Zone 34, located in the Lake Simcoe Watershed region (Lake Simcoe Region Conservation Authority 2018). The trees were potted on 3 Nov. 2017 into 16.5 cm wide × 17.5 cm deep pots using LiteWay® top soil [Premier Tech, Rivière-du-Loup, QC, Canada] mixed with sand [All Treat Farms, Arthur, ON, Canada] in a 1:13 ratio. When the plants were removed from the pots at the end of the study, we observed limited root growth.

Starting 16 Nov. 2017, the trees were left to overwinter at the Environmental Sciences Western field station outside of London, ON, Canada (43° 4' 29.5896" N, 81° 20' 14.8632" W). A layer of mulch was placed over the soil surface to prevent excessive soil freezing over the winter. Soil surface temperatures were measured with temperature loggers (LogTag Trix-8 Recorders, Auckland, New Zealand), and air temperatures in London, ON were collected from a local weather station (Environment Canada, National Climate Data and Information Archive). Soil temperatures averaged 0.2 °C and reached a minimum of -2.1 °C during the months of December and January, while air temperature averaged -5.8 °C and reached a low of -19.9 °C (Fig. S1).

The trees were removed from the field on 26 Feb. 2018 and placed in a greenhouse set at 20 °C day / 15 °C night, and the mulch was removed from the soil. The trees were watered regularly, but not fertilized, and they experienced a natural photoperiod; the greenhouse shaded an estimated 57 % of sunlight and the trees received an average daily maximum photosynthetically active radiation (PAR) of 1250 µmol photons m^{-2} s^{-1}. On 15 Mar. 2018, the trees were placed into a controlled environment chamber (Environmental Growth Chambers, Chagrin Falls, OH, USA) set at 10 °C day/night. The chamber was equipped with high-pressure sodium and metal halide lights and the trees were exposed to a photoperiod of 11 h with an irradiance of 1150 µmol photons m^{-2} s^{-1} at plant height. Each tree received 150 mL of water daily that was kept at a constant 10 °C.

Acclimation temperatures and N treatments

Beginning on 22 Mar. 2018, two trees per day were removed from the 10 °C chamber and placed into a 6 °C chamber; this process (movement of trees from the 10 °C chambers to the 6 °C) was completed after one week. This temperature shift was performed on half of the trees, which comprised the 6A treatment. The other half of the trees remained in the 10 °C chamber until gas exchange measurements were taken and comprised the 10A treatment. The 10A trees were considered to be non-acclimated and used as our controls. The chambers provided 11 h of photosynthetically active radiation (PAR = 1150 µmol photons m^{-2} s^{-1}) and were set at a constant target temperature and relative humidity of 60 %. Vapor pressure deficit (VPD) was 0.56 kPa in the 6 °C chamber and 0.74 kPa in the 10 °C chamber. During this acclimation period, the trees were subjected to their respective temperatures for six days and fertilized with either low N (LN; Hoagland's solution with 40 ml 1.0 M NH_4NO_3) or high N (HN; Hoagland's solution with 0 ml 1.0 M NH_4NO_3) (see Table S1 and Table S2 for the Hoagland's solution contents). Each tree received 50 mL of fertilizer on the second, fourth and sixth day of the acclimation treatment, and 50 mL of de-ionized water kept at the chamber temperature during the first, third and fifth day. In summary, there were two acclimation temperatures ($T_{acclimation}$; 6A and 10A) and two fertilization levels (LN or HN), resulting in four experimental treatment combinations. We measured 7 individuals per treatment combination (4 × 7 = 28 individuals total).

A/C_i, R_d, and temperature response curves

Following six days at $T_{acclimation}$, an individual tree (LN or HN) was removed and placed into a chamber set at 18 °C, where PAR = 1150 µmol photons m^{-2} s^{-1}. The trees were given 20–25 mins to adjust to the new chamber conditions and for the leaf temperature (T_{leaf}) to approach the desired value. Then, the response of net CO_2 assimilation rates (A_{net}) to changes in intercellular CO_2 concentrations (C_i) were assessed using a LI-6400 XT portable photosynthesis system (LI-COR, Lincoln, NE, USA). The LI-6400 XT was set to a constant flow of 300 µmols^{-1} and a PAR of 1000 µmol photons m^{-2} s^{-1} (10 % blue light), which was light-saturating based on prior photosynthetic light response curves (data not shown). Measurements were taken at CO_2 concentrations of 300, 200, 100, 50, 400, 400, 600, 800, 1000, 1200, 1600 and 2000 µmol mol^{-1} to generate the A/C_i curves. This was repeated at multiple T_{leaf} values (in order: T_{leaf} = 18, 14, 10, 6 and 2 ° C) by adjusting both the controlled environment chamber and cuvette temperature.

Cuvette relative humidity ranged from 48 % to 63 % and the leaf VPD was between 0.5 to 1.1 kPa over the leaf temperature range.

After measuring the A/C_i curves at a leaf temperature of 2 °C, the chamber lights were turned off and the LI-6400 XT was set to PAR = 0 µmol photons m^{-2} s^{-1}. Dark respiration (R_d) was determined after 10 mins when T_{leaf} = 2 °C. The chamber and cuvette temperatures were gradually ramped up to achieve a T_{leaf} of 6 °C, and R_d was determined after 10 min. This process was repeated for T_{leaf} values of 10, 14 and 18 °C. Two trees were successively measured in this way each day (i.e., the measurement of the trees were staggered over time).

We determined V_{cmax} and J_{max} from each A/C_i curve using a bilinear model. From there, we fit temperature response curves of V_{cmax} and J_{max} for each leaf. Curves were fit using a third-order polynomial as in O'Sullivan *et al*. (2013):

$$k_T = \exp (a + b*T_{leaf} + c*T_{leaf}^2) \quad \text{(Equation 1)}$$

where k_T (µmol m^{-2} s^{-1}) is the process rate (i.e., V_{cmax} or J_{max}) at a leaf temperature (T_{leaf}), a (µmol m^{-2} s^{-1}) corresponds to the exponential coefficient of k_T at T_{leaf} = 0 °C, b (µmol m^{-2} s^{-1}°C^{-1}) describes the change in process rate with temperature at 0 °C, and c (µmol m^{-2} s^{-1} °C^{-2}) describes the change in the shape of the curve as temperatures increase.

Specific leaf area (SLA) and leaf N

Each tree was removed from the chamber after the completion of gas exchange measurements. The leaf used for gas exchange was cut at the petiole-stem node and the surface area was determined using a LI-3200C leaf area meter (LI-COR, Lincoln, NE, USA) and dried in an oven at 60 °C for 3 d. After drying, leaves were weighed and the specific leaf area (SLA; m^2 g^{-1}) was calculated as the leaf area divided by the dry leaf mass. Total leaf N concentration (N_{mass}; g g^{-1}) was determined for each leaf through combustion using a Costech 4010 (Costech Analytical Technologies, Valencia, CA, USA). Leaf N was converted to a per area basis (N_{area}; g m^{-2}) using the SLA.

We used SLA to calculate A_{net}, V_{cmax}, J_{max}, and R_d on per dry weight (DW) bases (i.e., µmol g^{-1} s^{-1}), indicated using the subscript $_{/DW}$ (e.g., $A_{net/DW}$ for net CO_2 assimilation rates per unit dry mass). We used N_{area} to calculate A_{net}, V_{cmax}, J_{max}, and R_d on per gram N basis (i.e.,

μmol g N^{-1} s^{-1}), indicated using the subscript $_{/N}$ (e.g., $A_{net/N}$ for net CO_2 assimilation rates per gram of leaf N).

Statistical analyses

Two-way ANOVA models were used to assess the treatment effects ($T_{acclimation}$, N treatment, and their interaction) on SLA and leaf N expressed on a leaf mass (N_{mass}) and leaf area (N_{area}) basis.

Generalized linear mixed models were used to assess treatment effects (T_{leaf}, $T_{acclimation}$, N treatment, and their interactions) on A_{net}, $A_{net/N}$, $A_{net/DW}$, stomatal conductance (g_s; mmol m^{-2} s^{-1}), and the C_i/C_a ratio at atmospheric CO_2 concentrations of 400 ppm and 2000 ppm. In the models, tree ID was included as a random factor to account for the repeated measures structure. Subsequently, an ANOVA test was performed to determine the significance of the fixed factors in the mixed model. We further examined the effects of $T_{acclimation}$, N treatment, and their interaction on A_{net} at CO_2 concentrations of 400 ppm and 2000 ppm when $T_{leaf} = T_{acclimation}$ using two-way ANOVAs.

Generalized linear mixed models were also used to assess the effects of T_{leaf}, $T_{acclimation}$, N treatment, and their interactions on V_{cmax}, $V_{cmax/N}$, $V_{cmax/DW}$, J_{max}, $J_{max/N}$, $J_{max/DW}$, R_d, $R_{d/N}$, and $R_{d/DW}$. In the models, tree ID was included as a random factor to account for the repeated measures structure. Subsequently, an ANOVA test was performed to determine the significance of the fixed factors for each mixed model. We further examined the effects of $T_{acclimation}$, N treatment, and their interaction on V_{cmax}, $J_{max,}$ the ratio between J_{max}/V_{cmax} (JV), and R_d when $T_{leaf} = T_{acclimation}$ using two-way ANOVAs. In addition, we determined the treatment effects ($T_{acclimation}$, N, and their interaction) on parameters a, b and c in Eqn. 1 for V_{cmax}, J_{max} and R_d using two-way ANOVAs.

Throughout, percent differences were calculated as:

$$\frac{(\text{Higher Value})-(\text{Lower Value})}{(\text{Lower Value})} \times 100 \qquad \text{(Equation 2)}$$

Residuals were assessed visually for violations of homogeneity and normality. $V_{cmax/N}$ and $J_{max/N}$ were squared and $R_{d/DW}$ was square-root transformed to normalize the residuals;

transformations were selected by running through a series of Shapiro-Wilks tests on logarithmic, square root, and squared data. The analyses were run in R version 3.6.0 (R Core Development) with the packages 'plantecophys' (Duursma 2015) for A-Ci curve fitting. The "lm" function in base R was used for linear model fitting. The "lmer" function in the "lme4" package (Bates *et al.* 2014) was used for generalized linear mixed model fitting. The "Anova" function in the "car" package (Fox *et al.* 2016) was used for ANOVA tests. The packages "eemeans" (Lenth *et al.* 2020) and "multcomp" (Hothorn *et al.* 2008) were used to compare means within a given treatment using Tukey's tests and an $\alpha = 0.05$. Symbols have been defined in Table 1.

RESULTS

Leaf N and SLA

Leaf N_{area} was 10 % greater in the HN trees relative to the LN trees, but there was no $T_{acclimation}$ effect on N_{area} (Fig. 1a; Table S3). Leaf N_{mass} was 20 % greater in HN compared to LN trees, and 25 % greater in 6A trees than in 10A trees (Table S3). The N treatment did not affect SLA, but SLA was 17 % greater in 6A relative to 10A trees (Fig. 1b; Table S3).

Instantaneous temperature response curves: A_{400}

Net CO_2 assimilation rates measured at 400 ppm CO_2 (A_{400}) were 63 % greater in 10A trees than in 6A trees. When T_{leaf} was 18 °C, the 10A trees had 91 % greater A_{400} than the 6A trees, and when T_{leaf} was 14 °C, the 10A trees had 66 % greater A_{400} than 6A trees (based on averages across both the LN and HN treatments). A significant T_{leaf} by $T_{acclimation}$ interaction (Table 2) indicated that the effects of $T_{acclimation}$ were most apparent at high T_{leaf} (14–18 °C). While the N treatment did not alter A_{400} or the response of A_{400} to $T_{acclimation}$, it did affect the thermal sensitivity of A_{400}, with the HN trees showing a less steep increase in A_{400} with rising T_{leaf} than the LN trees (Fig. 2a, b; Table 2). When assessed at their respective $T_{acclimation}$, 10A trees had higher A_{400} than 6A trees (Fig. 2a, b; Table 3). Because the LN trees had similar A_{400} as the HN trees, but lower N_{area}, LN trees had 52 % higher $A_{400/N}$ than HN trees (Fig. S2; Table S4). Despite the effect of $T_{acclimation}$ on SLA, the A_{400} results were similar on both a leaf area and dry weight basis (Table S4).

Stomatal conductance at 400 ppm CO_2 (g_{s400}) was 56 % higher in 10A trees than in 6A trees, and the N treatments had no effect on g_{s400} (Table 2). The g_{s400} increased at higher T_{leaf} for 10A trees, but not for 6A trees (Fig. 2c, d; Table 2). The C_i/C_a decreased with increasing T_{leaf} (Fig. 2e, f), but was not influenced by $T_{acclimation}$ or the N treatments (Table 2).

Instantaneous temperature response curves: A_{2000}

Net CO_2 assimilation rates measured at 2000 ppm CO_2 (A_{2000}) did not differ between the HN and LN trees (Table 2). A_{2000} increased with higher T_{leaf}, and this effect was more pronounced in 10A trees compared to 6A trees (Fig. 3a, b), though there was no $T_{leaf} \times$ N treatment interaction for A_{2000} (Table 2).

When A_{2000} was measured at $T_{acclimation}$, 10A trees had higher A_{2000} than 6A trees (Fig. 3a, b; Table 3). In addition, the 10A trees measured at a T_{leaf} of 10 °C had higher $A_{2000/N}$ than the 6A trees measured at a T_{leaf} of 6 °C (Fig. S3; Table S5). The A_{2000} results were similar on both a leaf area and dry weight basis, except that there was no $T_{acclimation} \times T_{leaf}$ interaction on a dry weight basis (Table S4). The A_{2000} was similar in 10A trees relative to 6A trees at higher T_{leafs} when dry weight was accounted for (Fig. S3).

Stomatal conductance at 2000 ppm CO_2 (g_{s2000}) was 52 % greater in 10A compared to 6A trees, and g_{s2000} increased with increasing T_{leaf} in 10A trees, but decreased at higher T_{leaf} in 6A trees (Fig. 3c, d; Table 2). The C_i/C_a ratio decreased with increasing T_{leaf}, and this decline was more pronounced in 6A trees relative to 10A trees (Fig. 3e, f; Table 2).

Instantaneous temperature response curves: V_{cmax}, J_{max}, R_d

V_{cmax} was greater at higher T_{leaf} (Fig. 4a, b), however there were no differences in V_{cmax} between the N or $T_{acclimation}$ treatments (Table 4). When $T_{leaf} = T_{acclimation}$, 10A trees had higher V_{cmax} relative to 6A trees (Fig. 4a, b), but rates were unaffected by the N treatments (Table 3). When measured at $T_{acclimation}$, $V_{cmax/N}$ was 27 % higher in the LN trees compared to HN trees (Fig. S4; Table S5). None of the parameters describing the thermal response of V_{cmax} were significantly altered by any of the treatments (Table 5).

J_{max} was stimulated by increasing T_{leaf} (Fig. 4c, d), but there were no differences in J_{max} between the N or $T_{acclimation}$ treatments (Table 4). When $T_{leaf} = T_{acclimation}$, 10A trees had higher J_{max} relative to 6A trees (Fig. 4c, d; Table 2). When expressed on a leaf N basis, the LN trees had

29 % higher $J_{max/N}$ than the HN trees, and there was a significant interaction where T_{leaf} had a greater effect for the LN trees compared to the HN trees (Fig. S5; Table S6). When $T_{leaf} = T_{acclimation}$, 10A trees had higher J_{max} (Fig. 4c, d; Table 3), $J_{max/N}$ (Fig. S5; Table S5) and $J_{max/DW}$ (Fig. S5; Table S5) relative to 6A trees. Furthermore, when measured at their respective $T_{acclimation}$ values, there was also a significant N effect on $J_{max/N}$, where the rates were 29 % higher in the LN treatment compared to the HN treatment (Fig. S5; Table S5). The treatments did not affect the parameters describing the thermal response of J_{max} (Table 5).

Increasing T_{leaf} significantly reduced the ratio between J_{max} and V_{cmax}, where JV was 17 % lower in trees measured at leaf temperatures of 18 °C relative to 2 °C (Table S7). The 10A trees had lower a J/V relative to the 6A trees when the trees were assessed at their $T_{acclimation}$, but there were no N treatment effects on J/V measured at $T_{acclimation}$ (Table S8). The rates of R_d increased with increasing T_{leaf} but were not altered by $T_{acclimation}$ or N (Fig. 4e, f; Table 4). There were also no treatment effects on R_d when $T_{leaf} = T_{acclimation}$ (Fig. 4e, f; Table 3).

DISCUSSION

Thermal acclimation of net CO_2 assimilation rate was determined by stomatal conductance

A greater stomatal conductance in the 10A trees as compared to the 6A trees increased A_{net} at high T_{leaf} despite the relative insensitivity of g_s to T_{leaf}. This demonstrates the non-linear effect of g_s on A_{net} as leaf temperatures change: the benefit of a high g_s increases as T_{leaf} increases. Because it is more difficult, and likely more costly (Roderick and Berry 2001; Franks and Brodribb 2005; Prentice *et al.* 2014), to transport water at low temperatures, trees acclimated to low temperatures tend to operate at low stomatal conductance (Paillassa *et al.* 2020). Low temperatures increase water viscosity and decrease cell permeability and root water transport, both of which can reduce g_s (Jensen and Taylor 1961; Fredeen and Sage 1999). For example, for various woody and herbaceous species, water uptake and transpiration at low temperatures were reduced, and species from cooler climates were found to maintain higher rates of water uptake at low soil temperatures (<5 °C) compared to species from warmer regions (Kramer 1942). In addition, rice plants exposed to low root temperatures had decreased conductance in shoots, though increased aquaporin expression may have offset this decreased water flow (Sakurai *et al.* 2005; Murai-Hatano *et al.* 2008; Kuwagata *et al.* 2012). The insensitivity of stomatal conductance to changes in T_{leaf} may have been related to the small changes in VPD over the T_{leaf}

range (0.5–1.1 KPa); stomatal conductance was also insensitive to T_{leaf} changes between 15 and 25 °C in a previous study on *Populus balsamifera* trees (Silim *et al.* 2010).

At an external CO_2 concentration of 2000 ppm, there was an interaction between T_{leaf} and $T_{acclimation}$, and the decline in C_i:C_a with increasing temperature was more pronounced in the 6A than in the 10A trees. Therefore, rapidly decreasing intercellular CO_2 concentrations at higher leaf temperatures likely reduced A_{net} in the 6A trees more than in the 10A trees. Interestingly, the acclimation by leaf temperature interaction was not observed for $A_{2000/DW}$, although it was observed for $A_{2000/N}$ and A_{2000}. It is possible that leaf growth and biomass accumulation was greater in 10A trees relative to in 6A trees during the acclimation period, causing this difference. This would mean that 10A trees had greater A_{2000} values at high leaf temperatures and biomass accumulation than 6A trees.

Photosynthetic and respiration capacity showed no temperature acclimation

We saw no effect of $T_{acclimation}$ on the biochemical parameters V_{cmax} or J_{max}. Instead, the only response observed was the direct effect of T_{leaf} on net photosynthesis. This directly contradicts a number of previous studies of photosynthetic temperature acclimation (Kattge and Knorr 2007; Campbell *et al.* 2007; Gunderson *et al.* 2010; Crous *et al.* 2013; Smith and Dukes, 2013; Way and Yamori 2014; Yamori *et al.* 2014; Scafaro *et al.* 2017; Smith and Dukes 2017; Dusenge *et al.* 2018; Reich *et al.* 2018; Kumarathunge *et al.* 2019; Smith *et al.* 2019; Stefanski *et al.* 2020; but see Smith *et al.* 2020). The one possible signal of biochemical acclimation that we did observe was a decrease in the JV ratio with increased acclimation temperatures. This has been commonly observed in other species (Kattge *et al.* 2007; Way and Sage 2008; Smith and Dukes 2017; Smith and Dukes 2018; Kumarathunge *et al.* 2019) and has been attributed to differences in the sensitivity of V_{cmax} and J_{max} to temperature (Hikosaka *et al.* 2006) or increased relative investment in carboxylation to counteract increased photorespiration at high temperatures (Smith *et al.* 2019). Nonetheless, our results suggest that increasing leaf temperatures may increase V_{cmax} and J_{max} in *Populus balsamifera*, but acclimation temperature has minimal impacts on these parameters.

Furthermore, we saw no effect of $T_{acclimation}$ on R_d, though acclimation of leaf respiration has been observed in many tree species (Slot and Kitajima 2015), including *Populus balsamifera* (Silim *et al.* 2010), and *Populus* maximowiczii × *Populus nigra* (Benomar *et al.* 2019). It may be

expected that the trees acclimated to lower temperatures would have greater respiratory capacity than the trees acclimated to higher temperatures to limit feedback inhibition of photosynthesis (Atkin and Tjoelker 2003). However, thermal acclimation of respiration is not always observed in plants (Crous *et al.* 2017). Marginal differences were observed between the trees acclimated to 6 and 10 °C when the respiration rates were standardized by N and measured at $T_{leaf} = T_{acclimation}$, but these differences were a result of direct temperature effects on respiration capacity.

Soil nitrogen had little impact on temperature acclimation

The N treatments had little effect on the photosynthetic or respiratory parameters measured in our trees. While the HN trees had greater N_{area} than LN trees, the lack of an impact of the N treatments on photosynthesis or respiration indicated that the added leaf N was not contributing substantially to leaf carbon exchange processes, and thus not impacting thermal acclimation. However, it is possible that the short treatment period may not have allowed for enough time for acclimation to occur. Smith and Dukes (2017) found that seven days was long enough for photosynthetic thermal acclimation to occur in a number of different species. However, the lowest temperature they acclimated the plants to was 15 °C (Smith and Dukes 2017). In our study, it is possible that low temperatures limited xylem water transport rates of nutrients needed for acclimation to occur (Franks and Brodribb 2005), though the changes seen in N_{area} between the N treatments implies this is not likely. Additionally, previous studies have shown that temperature acclimation is greater in leaves that develop at the new temperature than those that do not (Campbell *et al.* 2007). Similar studies using longer acclimation time periods are needed to further elucidate the effect of the timescale of acclimation. Nonetheless, the lack of response of leaf biochemistry to $T_{acclimation}$ indicates that the acclimation of A_{net} to low temperatures was directly due to changes in stomatal conductance.

Populus species depend on N stored in the fall for plant growth in the subsequent spring, and bark storage proteins are often broken down and used for photosynthesis during the spring (Rennenberg *et al.* 2010). Thus, our trees may have had sufficient amounts of N from internal sources, which may explain why our N treatments had minimal impacts on photosynthesis and respiration. However, our N treatments were effective on many other parameters (e.g., N_{mass} and N_{area}).

Low temperature-acclimated leaves had the highest SLA

Specific leaf area has been observed to increase with higher acclimation temperatures (Way and Oren 2010). For example, this trend was observed in *Populus* spp. (Benomar *et al.* 2019) and *Corymbia calophylla* (Aspinwall *et al.* 2017). A decrease in SLA can compensate for the low enzymatic activity at cool temperatures by increasing the density of photosynthetic enzymes per area (Kuwagata *et al.* 2012). In our study, the 6A trees instead had the highest SLA, indicating a decrease in leaf density per unit area relative to the 10A trees. This SLA response was unexpected given that the acclimation period was only six days long, and the leaves were developed and expanded prior to that time. However, the effect of acclimation temperature on SLA (17%) was relative minor.

TBMs predictions at low temperatures

Terrestrial carbon cycling models simulate photosynthetic temperature acclimation via adjustments in the instantaneous thermal response of V_{cmax} and J_{max} with changes in acclimation temperature (Smith and Dukes 2013). We did not find evidence of this mechanism. Nonetheless, our results do not differ from the commonly used KK 2007 model at low temperatures. Both our data and the KK 2007 model indicate little acclimation of J_{max} and V_{cmax} at low leaf temperatures. This suggests that the KK 2007 model could be extended to lower temperatures, as has been recently suggested elsewhere (Kumarathunge *et al.* 2019). Our data do, however, suggest that thermal acclimation of stomatal conductance is an important process for models to consider, particularly for low temperatures. Currently, most terrestrial carbon cycling models do not simulate thermal acclimation of stomatal conductance (Smith and Dukes 2013). However, a growing body of evidence suggests that stomatal conductance changes with acclimation temperature (Prentice *et al.* 2014; Lin *et al.* 2015; Wang *et al.* 2017; Dusenge *et al.* 2020), similar to the results we observed. Indeed, models exist to implement this response (Medlyn *et al.* 2011; Wang *et al.* 2017), which have been included in carbon cycling models (e.g., Stocker *et al.* 2019). Finally, our results do not indicate that short-term N availability has any impact on photosynthetic temperature acclimation simplifying modeling efforts. However, future studies should investigate the link between longer-term N availability and acclimation of photosynthetic capacity.

Climate warming in historically cold regions

Boreal regions experience an average temperature below 10 °C for 9 to 11 months of the year (Belda *et al*. 2014). Summers are typically short and mean annual temperatures can range from -10 to 5.5 °C in boreal regions of North America (Hall *et al*. 2004). Climate change has increased air temperatures globally, and these changes are expected to be greater for boreal regions, where some models predict temperature increases of 4–10 °C (Sala *et al*. 2000; Brown and Caldeira 2017). Based on our results, climate warming can potentially improve the physiological functioning of plants growing at low temperatures (<11 °C). An increase in leaf temperature of 4 °C, for example, can increase carbon assimilation, maximum carboxylation rates, and electron transport for both trees acclimated to 6 °C and 10 °C. Our results also may have important implications for non-boreal regions; for example, temperate regions generally experience an average temperature below 10 °C for 5 to 8 months of the year (Belda *et al*. 2014), and an increase in photosynthetic capacity may increase nutrition acquisition in both the fall and spring. However, studies on larger trees are needed to confirm these results across life stage.

Conclusions

We set out to determine whether thermal acclimation of photosynthesis to low temperatures was affected by short-term soil N availability. Carbon assimilation was greater in the 10A trees than the 6A trees, which was attributed to higher stomatal conductance in the 10A trees. Increased N supply did not influence thermal acclimation at these low temperatures. Understanding how widespread species, including *Populus balsamifera*, adjust to changes in air temperature will improve our predictions of CO_2 uptake in forests. Cold-acclimated ecotypes on the northern edge of habit may be subjected to warmer temperatures, which may enhance C uptake in the atmosphere as these trees acclimate. In contrast, periods of extended cold can reduce CO_2 uptake unless these trees are able to acclimate. Given the abundance of this species, there can be major consequences of thermal acclimation on the C cycle.

ACKNOWLEDGEMENTS

We would also like to thank the Natural Sciences and Engineering Research Council of Canada (NSERC) for awarding Discovery Grants to HALH and DAW, and an Alexander Graham Bell Canada Graduate Scholarship (CGS-D3) to RSK; DAW was also supported in part by the United

States Department of Energy contract No. DE-SC0012704 to Brookhaven National Laboratory. In addition, NGS acknowledges support from Texas Tech University. We would also like to thank David Michels for his assistance during this experiment.

CONFLICTS OF INTEREST

The authors declare that there no conflicts of interest.

AUTHOR CONTRIBUTIONS

RSK and NGS conceived the initial research questions. RSK, NGS, DAW and HALH contributed to the design of the study. RSK and NGS were responsible for the collection and statistical analysis of the data. RSK, NGS, DAW and HALH contributed to the interpretation of the data and writing of the manuscript. Data is available at Zenodo and be accessed using the DOI: 10.5281/zenodo.3958688.

REFERENCES

Ali AA, Xu C, Rogers A, McDowell NG, Medlyn BE, Fisher RA, Wullschleger SD, Reich PB, Vrugt JA, Bauerle WL, Santiago LS, Wilson CJ (2015) Global-scale environmental control of plant photosynthetic capacity. *Ecological Applications* **25**, 2349–2365.

Aspinwall M, Vårhammar A, Blackman C, Tjoelker M, Ahrens C, Byrne M, Rymer P (2017) Adaptation and acclimation both influence photosynthetic and respiratory temperature responses in *Corymbia calophylla*. *Tree Physiology* **37**, 1095–1112.

Atkin OK, Edwards EJ, Loveys BR (2000) Response of root respiration to changes in temperature and its relevance to global warming. *New Phytologist* **147**, 141–154.

Atkin OK, Tjoelker MG (2003) Thermal acclimation and the dynamic response of plant respiration to temperature. *Trends in Plant Science* **8**, 343–351.

Atkin OK, Atkinson LJ, Fisher RA, Campbell CD, Zaragoza-Castells J, Pitchford JW, Woodward FI, Hurry V (2008) Using temperature-dependent changes in leaf scaling relationships to quantitatively account for thermal acclimation of respiration in a coupled global climate–vegetation model. *Global Change Biology*, **14**, 2709–2726.

Bates D, Maechler M, Bolker B, Walker S (2014) lme4: Linear mixed-effects models using Eigen and S4. R package version 1.1–7. http://CRAN.R-project.org/package=lme4.

Bates D, Maechler M, Bolker B, Walker S (2015) Fitting linear mixed-effects models using lme4. *Journal of Statistical Software* **67**, 1-48.

Beer C, Reichstein M, Tomelleri E, Ciais P, Jung M, Carvalhais N, Rödenbeck C, Arain MA, Baldocchi D, Bonan GB, Bondeau A, Cescatti A, Lasslop G, Lindroth A, Lomas M, Luyssaert S, Margolis H, Oleson KW, Roupsard O, Veenendaal E, Viovy N, Williams C, Woodward FI, Papale D (2010) Terrestrial gross carbon dioxide uptake: global distribution and covariation with climate. *Science* **329**, 834–838.

Belda M, Holtanová E, Halenka T, Kalvová J (2014) Climate classification revisited: from Köppen to Trewartha. *Climate Research* **59**, 1–13.

Benomar L, Moutaoufik MT, Elferjani R, Isabel N, DesRochers A, Guellab AE, Khlifa R, Hassania LAI (2019) Thermal acclimation of photosynthetic activity and RuBisCO content in two hybrid poplar clones. *PLoS ONE* **14**, e0206021.

Brown PT, Caldeira K (2017) Greater future global warming inferred from Earth's recent energy budget. *Nature* **552**, 45–50.

Campbell C, Atkinson L, Zaragoza-Castells J, Lundmark M, Atkin O, Hurry V (2007) Acclimation of photosynthesis and respiration is asynchronous in response to changes in temperature regardless of plant functional group. *New Phytologist* **176**, 375–389.

Chapin FS III, Shaver GR (1996) Physiological and growth responses of Arctic plants to a field experiment simulating climatic change. *Ecology* **77**, 822–840.

Ciais P, Sabine C, Bala G, Bopp L, Brovkin V, Canadell J, Chhabra A, DeFries R, Galloway J, Heimann M, Jones C, Le Quéré C, Myneni RB, Piao S, Thornton P (2013) Climate change 2013: the physical science basis. Contribution of Working Group I to the fifth assessment report of the Intergovernmental Panel on Climate Change. In: Stocker TF, Qin D, Plattner G-K, Tignor M, Allen SK, Boschung J, Nauels A, Y Xia, Bex V, and Midgley PM, eds. Carbon and other biogeochemical cycles. Cambridge, UK & New York, NY, USA: Cambridge University Press, 1535.

Crous KY, Quentin AG, Lin Y-S, Medlyn BE, Williams DG, Barton CVM, Ellsworth DS (2013) Photosynthesis of temperate *Eucalyptus globulus* trees outside their native range

has limited adjustment to elevated CO_2 and climate warming. *Global Change Biology* 19, 3790–3807.

Crous KY, Wallin G, Atkin OK, Uddling J, af Ekenstam A (2017) Acclimation of light and dark respiration to experimental and seasonal warming are mediated by changes in leaf nitrogen in *Eucalyptus globulus*. *Tree Physiology* **37**, 1069–1083.

Cohen J, Pfeiffer K, Francis JA (2018) Warm Arctic episodes linked with increased frequency of extreme winter weather in the United States. *Nature Communications* **9,** 869.

Dusenge ME, Duarte AG, Way DA (2019) Plant carbon metabolism and climate change: elevated CO_2 and temperature impacts on photosynthesis, photorespiration and respiration. *New Phytologist* **221**, 32–49.

Dusenge ME, Madhavji S, Way DA (2020) Contrasting acclimation responses to elevated CO_2 and warming between an evergreen and a deciduous boreal conifer. *Global Change Biology* **26**, 3639–3657.

Duursma, RA (2015) Plantecophys - An R package for analysing and modelling leaf gas exchange data. *PLoS ONE* **10**, e0143346.

Environment Canada, National Climate Data and Information Archive. https://climate.weather.gc.ca/

Evans JR, Seeman JR (1989) The allocation of protein nitrogen in the photosynthetic apparatus: costs, consequences, and control. In: Briggs W, eds. Photosynthesis. Alan R. Liss, New York, NY, 183–205.

Fox J, Weisberg S, Adler D, Bates D, Baud-Bovy G, Ellison S, Firth D, Friendly M, Gorjanc G, Graves S, Heiberger R, Krivitsky P, Laboissiere R, Maechler M, Monette G, Murdoch D, Nilsson H, Ogle D, Ripley B, Venables W, Walker S, Winsemius D, Zeileis A (2016) *Package 'Car'*. http://cranr.project.org/web/packages/car/car.pdf

Franks P, Brodribb TJ (2005) Stomatal control and water transport in the xylem. In: Holbrook NM, Zwieniecki MA, eds. Vascular transport in plants. Elsevier Academic Press, Amsterdam, Netherlands, 69–89.

Fredeen A, Sage R (1999) Temperature and humidity effects on branchlet gas-exchange in whitespruce: an explanation for the increase in transpiration with branchlet temperature. *Trees* **14**, 161–168.

Galloway JN, Dentener F, Capone DG, Boyer EW, Howarth RW, Seitzinger SP, Asner GP, Cleveland CC, Green PJ, Holland EA, Karl DM, Michaels AF, Porter JH, Townsend AR, Vöosmarty CJ (2004) Nitrogen cycles: past, present, and future. *Biogeochemistry* **70**, 153–226.

Gu L, Hanson PJ, Post WM, Kaiser DP, Yang B, Nemani R, Pallardy SG, Meyers T (2008) The 2007 eastern US spring freeze: increased cold damage in a warming world? *BioScience* **58**, 253–262.

Gunderson CA, O'hara KH, Campion CM, Walker AV, Edwards NT (2010) Thermal plasticity of photosynthesis: the role of acclimation in forest responses to a warming climate. *Global Change Biology* **16**, 2272–2286.

Hall FG, Betts AK, Frolking S, Brown R, Chen JM, Chen W, Halldin S, Lettenmaier DP, Schafer J (2004) The Boreal Climate. In: Kabat P *et al.* eds. Vegetation, Water, Humans and the Climate. Global Change — The IGBP Series. Springer, Berlin, Heidelberg, 93–161.

Heskel MA, O'Sullivan OS, Reich PB, Tjoelker MG, Weerasinghe LK, Penillard A, Egerton JJ, Creek D, Bloomfield KJ, Xiang J, Sinca F, Stangl ZR, Martínez-de la Torre A, Griffin KL, Huntingford C, Hurry V, Meir P, Turnbull M, Atkin OK (2016) Convergence in the temperature response of leaf respiration across biomes and plant functional types. *Proceedings of the National Academy of Sciences of the United States of America* **113**, 3832–3837.

Hikosaka K, Ishikawa K, Borjigidai A, Muller O, Onoda Y (2006) Temperature acclimation of photosynthesis: mechanisms involved in the changes in temperature dependence of photosynthetic rate. *Journal of Experimental Botany* **57**, 291–302.

Hothorn T, Bretz F, Westfall P (2008) Simultaneous inference in general parametric models. *Biometrical Journal* **50**, 346–363.

Jensen RD, Taylor SA (1961) Effect of temperature on water transport through plants. *Plant Physiology* **36**, 639–642.

Kattge J., Knorr W (2007) Temperature acclimation in a biochemical model of photosynthesis: a reanalysis of dat from 36 species. *Plant, Cell and Environment* **30**, 1176–1190.

Kramer PJ (1942) Species differences with respect to water absorption at low soil temperatures. *American Journal of Botany* **29**, 828–832.

Kumarathunge DP, Medlyn BE, Drake JE, Tjoelker MG, Aspinwall MJ, Battaglia M, Cano FJ, Carter KR, Cavaleri MA, Cernusak LA, Chambers JQ, Crous KY, De Kauwe MG, Dillaway DN, Dreyer E, Ellsworth DS, Ghannoum O, Han Q, Hikosaka K, Jensen AM, Kelly JWG, Kruger EL, Mercado LM, Onoda Y, Reich PB, Rogers A, Slot M, Smith NG, Tarvainen L, Tissue DT, Togash HF, Tribuzy ES, Uddling J, Vårhammar A, Wallin G, Warren JM, Way DA (2019) Acclimation and adaptation components of the temperature dependence of plant photosynthesis at the global scale. *New Phytologist* **222**, 768–784.

Kumarathunge DP, Drake JE, Tjoelker MG, López R, Pfautsch S, Vårhammar A, Medlyn BE (2020) The temperature optima for tree seedling photosynthesis and growth depend on water inputs. *Global Change Biology*, **26**, 2544–2560.

Kuwagata T, Ishikawa-Sakurai J, Hayashi H, Nagasuga K, Fukushi K, Ahamed A, Takasugi K, Katsuhara M, Murai-Hatano M (2012) Influence of low air humidity and low root temperature on water uptake, growth and aquaporin expression in rice plants. *Plant & Cell Physiology* **53**, 1418–1431.

Lake Simcoe Region Conservation Authority (2018) Adapting forestry programs to climate change. https://www.lsrca.on.ca/Shared%20Documents/reports/Adapting-ForestryPrograms-for-Climate-Change.pdf

Lenth R, Singmann H, Love J, Buerkner P, Herve M (2020) Package 'emmeans'. https://cran.r-project.org/web/packages/emmeans/index.html

Lin Y, Medlyn BE, Duursma, RA, Prentice IC, Wang H, Baig S, Eamus D, Dios VR, Mitchell PJ, Ellsworth DS, De Beeck MO, Wallin G, Uddling J, Tarvainen L, Linderson ML, Cernusak LA, Nippert JB, Ocheltree TW, Tissue DT, Martin-StPaul NK, Rogers A, Warren JM, De Angelis P, Hikosaka K, Han Q, Onoda Y, Gimeno TE, Barton CVM, Bennie J, Bonal D, Bosc A, Löw M, Macinins-Ng C, Rey A, Rowland L, Setterfield SA, Tausz-Posch S, Zaragoza-Castells J, Broadmeadow MSJ, Drake JE, Freeman M, Ghannoum O, Hutley LB, Kelly JW, Kikuzawa K, Kolari P, Koyama K, Limousin JM, Meir P, Lola da Costa AC, Mikkelsen TN, Salinas N, Sun W, Wingate L (2015) Optimal stomatal behaviour around the world. *Nature Climate Change* ***5***, 459 – 464.

Lombardozzi DL, Bonan GB, Smith NG, Dukes JS, Fisher RA (2015) Temperature acclimation of photosynthesis and respiration: a key uncertainty in the carbon cycle climate feedback. *Geophysical Research Letters* **42**, 8624–8631.

Mathur S, Agrawal D, Jajoo A (2014) Photosynthesis: response to high temperature stress. *Journal of Photochemistry and Photobiology B: Biology* **137**, 116–126.

Medlyn BE, Duursma RA, Eamus D, Llsworth DS, Prentice IC, Barton CVM, Crous KY, De Angelis P, Freeman M, Wingate L (2011) Reconciling the optimal and empirical approaches to modelling stomatal conductance. *Global Change Biology* **17**, 2134–2144.

Mercado LM, Medlyn BE, Huntingford C, Oliver RJ, Clark DB, Sitch S, Zelazowski P, Kattge J, Harper AB, Cox PM (2018) Large sensitivity in land carbon storage due to geographical and temporal variation in the thermal response of photosynthetic capacity. *New Phytologist* **218**, 1462–1477.

Murai-Hatano M, Kuwagata T, Sakurai J, Nonami H, Ahamed A, Nagasuga K, Matsunami T, Fukushi K, Maeshima M, Okada M (2008) Effect of low root temperature on hydraulic conductivity of rice plants and the possible role of aquaporins. *Plant and Cell Physiology* **49**, 1294–1305.

Nunes M, Ramalho J, Dias M (1993) Effect of nitrogen supply on the photosynthetic performance of leaves from coffee plants exposed to bright light. *Journal of Experimental Botany* **44**, 893–899.

O'Sullivan OS, Weerasinghe KWLK, Evans JR, Egerton JJG, Tjoelker M, Atkin OK (2013**)** High-resolution temperature responses of leaf respiration in snow gum (*Eucalyptus pauciflora*) reveal high-temperature limits to respiratory function. *Plant, Cell & Environment* **36**, 1268–1284.

Overland J, Dunlea E, Box J, Corell R, Forsinus M, Kattsov V, Olsen MS, Pawlak J, Reirson L-O, Wang M (2019) The urgency of arctic change. *Polar Science* **21**, 6–13.

Ow LF, Griffin KL, Whitehead D, Walcroft AS, Turnbull MH (2008) Thermal acclimation of leaf respiration but not photosynthesis in *Populus deltoides* x *nigra*. *New Phytologist* **178**, 123–134.

Paillassa J, Wright IJ, Prentice IC, Pepin S, Smith NG, Ethier G, Westerband A, Lamarque LJ, Wang H, Cornwell WK, Maire V (2020) When and where soil is important to modify the carbon and water economy of leaves. *New Phytologist* **228**, 121–135.

Peterson EB, Peterson NM (1992) Ecology, management, and use of aspen and balsam poplar in the prairie provinces. Forestry Canada, Northwest Region, Northern Forestry Centre, Edmonton, Alberta. Special Report 1.

Prentice IC, Dong N, Gleason SM, Maire V, Wright IJ (2014) Balancing the costs of carbon gain and water transport: testing a new theoretical framework for plant functional ecology. *Ecology Letters* **17**, 82–91.

Reich PB, Sendall KM, Stefanski A, Rich RL, Hobbie SE, Montgomery RA (2018) Effects of climate warming on photosynthesis in boreal tree species depend on soil moisture. *Nature* **562**, 263–267.

Rennenberg H, Wildhagen H, Ehlting B (2010) Nitrogen nutrition of poplar trees. *Plant Biology* **12**, 275–291.

Roderick ML, Berry SL (2001) Linking wood density with tree growth and environment: a theoretical analysis based on the motion of water. *New Phytologist* **149**, 473–485.

Rogers A, Medlyn BE, Dukes JS, Bonan G, von Caemmerer S, Dietze MC, Kattge J, Leakey ADB, Mercado LM, Niinemets Ü, Prentice IC, Serbin SP, Sitch S, Way DA, Zaehle S. (2017*a*) A roadmap for improving the representation of photosynthesis in Earth system models. *New Phytologist* **213**, 22–42.

Rogers A, Serbin SP, Ely KS, Sloan VL, Wullschleger SD (2017*b*) Terrestrial biosphere models underestimate photosynthetic capacity and CO_2 assimilation in the Arctic. *New Phytologist* **216**, 1090–1103.

Rogers A, Serbin SP, Ely KS, Wullschleger SD (2019) Terrestrial biosphere models may overestimate Arctic CO_2 assimilation if they do not account for decreased quantum yield and convexity at low temperature. *New Phytologist* **223**, 167–179.

Rogers PC, Pinno BD, Šebesta J, Albrectsen BR, Li G, Ivanova N, Kusbach A, Kuuluvainen T, Landhäusser SM, Liu H, Myking T, Pulkkinen P, Wen Z, Kulakowski D (2020) A global view of aspen: Conservation science for widespread keystone systems. *Global Ecology Conservation* **21**, e00828.

Sakurai J, Ishikawa F, Yamaguchi T, Uemura M, Maeshima M (2005) Identification of 33 rice aquaporin genes and analysis of their expression and function. *Plant & Cell Physiology* 46, 1568–1577.

Sala OE, Chapin FS 3rd, Armesto JJ, Berlow E, Bloomfield J, Dirzo R, Huber-Sanwald E, Huenneke LF, Jackson RB, Kinzig A, Leemans R, Lodge DM, Mooney HA, Oesterheld M, Poff NL, Sykes MT, Walker BH, Walker M, Wall DH (2000) Global biodiversity scenarios for the year 2100. *Science* **287**, 1770–1774.

Scafaro AP, Xiang S, Long BM, Bahar NHA, Weerasinghe LK, Creek D, Evans JR, Reich PB, Atkin OK (2017) Strong thermal acclimation of photosynthesis in tropical and temperate wet-forest tree species: the importance of altered Rubisco content. *Global Change Biology* **23**, 2783–2800.

Silim SN, Ryan N, Kubien DS (2010) Temperature responses of photosynthesis and respiration in *Populus balsamifera* L.: acclimation versus adaptation. *Photosynth Research* **104**, 19–30.

Slot M, Kitajima K (2015) General patterns of acclimation of leaf respiration to elevated temperatures across biomes and plant types. *Oecologia* **177**, 885–900.

Smith NG, Dukes JS (2013) Plant respiration and photosynthesis in global-scale models: incorporating acclimation to temperature and CO_2. *Global Change Biology* **19**, 45–63.

Smith NG, Dukes JS (2017) Short-term acclimation to warmer temperatures accelerates leaf carbon exchange processes across plant types. *Global Change Biology* **23**, 4840–4853.

Smith NG, Dukes JS (2018) Drivers of leaf carbon exchange capacity across biomes at the continental scale. *Ecology* **99**, 1610–1620.

Smith NG, Keenan TF, Prentice IC, Wang H, Wright IJ, Niinemets Ü, Crous KY, Domingues TF, Guerrieri R, Yoko Ishida F, Kattge J, Kruger EL, Maire V, Rogers A, Serbin SP, Tarvainen L, Togashi H., Townsend PA, Wang M, Weerasinghe LK, Zhou S-X (2019) Global photosynthetic capacity is optimized to the environment. *Ecology Letters* **22**, 506-517.

Smith NG, Lombardozzi D, Tawfik A, Bonan G, Dukes JS (2017) Biophysical consequences of photosynthetic temperature acclimation for climate. *Journal of Advances in Modeling Earth Systems* **9**, 536–547.

Smith NG, Malyshev SL, Shevliakova E, Kattge J, Dukes JS (2016) Foliar temperature acclimation reduces simulated carbon sensitivity to climate. *Nature Climate Change* **6**, 407–411.

Smith NG, McNellis RE, Dukes JS (2020) No acclimation: instantaneous responses to temperature maintain homeostatic photosynthetic rates under experimental warming across a precipitation gradient in *Ulmus americana*. *Annals of Botany – Plants* **12**, plaa027.

Soolanayakanahally RY, Guy RD, Silim SN, Song M (2013) Timing of photoperiodic competency causes phenological mismatch in balsam poplar (*Populus balsamifera* L.). *Plant, Cell & Environment* **36**, 116–127.

Stefanski A, Bermudez R, Sendall KM, Montgomery RA, Reich PB (2020) Surprising lack of sensitivity of biochemical limitation of photosynthesis of nine tree species to open-air experimental warming and reduced rainfall in a southern boreal forest. *Global Change Biology* **26**, 746–759.

Stinziano JR, Bauerle WL, Way DA (2019) Modelled net carbon gain responses to climate change in boreal trees: impacts of photosynthetic parameter selection and acclimation. *Global Change Biology* **25**, 1445–1465.

Stocker BD, Wang H, Smith NG, Harrison SP, Keenan TF, Sandoval D, Davis T, Prentice IC (2019) P-model v1.0: An optimality-based light use efficiency model for simulating ecosystem gross primary production. *Geoscientific Model Development Discussions* **13**, 1–59.

Vitousek PM, Aber JD, Howarth RW, Likens GE, Matson PA, Schindler DW, Schlesinger WH and Tilman DG (1997) Human alteration of the global nitrogen cycle: sources and consequences. *Ecological Applications* **7**, 737–750.

Walker AP, Beckerman AP, Gu L, Kattge J, Cernusak LA, Domingues TF, Scales JC, Wohlfahrt G, Wullschleger SD, Woodward FI (2014) The relationship of leaf photosynthetic traits – V_{cmax} and J_{max} – to leaf nitrogen, leaf phosphorus, and specific leaf area: a meta-analysis and modeling study. *Ecology and Evolution* **4**, 3218–3235.

Wang H, Prentice IC, Keenan TF, Davis TW, Wright IJ, Cornwell WK, Evans B, Peng C (2017) Towards a universal model for carbon dioxide uptake by plants. *Nature Plants* **3**, 734–741.

Waugh DW, Sobel AH, Polvani LM (2017) What is the polar vortex and how does it influence weather? *Bulletin of the American Meteorological Society* **98**, 37–44.

Way DA, Sage RF (2008) Thermal acclimation of photosynthesis in black spruce [*Picea mariana* (Mill.) B.S.P.]. *Plant, Cell & Environment* **31**, 1250–1262.

Way DA, Oren R (2010) Differential responses to changes in growth temperature between trees from different functional groups and biomes: a review and synthesis of data. *Tree Physiology* **30**, 669–688.

Way DA, Yamori W (2014) Thermal acclimation of photosynthesis: on the importance of adjusting our definitions and accounting for thermal acclimation of respiration. *Photosynthesis Research* **119**, 89–100.

Yamori W, Hikosaka K, Way DA (2014) Temperature response of photosynthesis in C3, C4, and CAM plants: temperature acclimation and temperature adaptation. *Photosynthesis Research* **119**, 101–117.

FIGURE CAPTIONS

Fig. 1 Average leaf N per area (a) and specific leaf area (b) for *Populus balsamifera* trees acclimated at 6 or 10 °C for six days and fertilized with high (HN) or low nitrogen (LN) Hoagland's solution (Table S1 and S2). The upper whisker represents the 90^{th} percentile, while the lower represents the 10^{th} percentile. The lower box boundary indicates the 25^{th} percentile and the upper box boundary indicates the 75^{th} percentile with the horizontal line indicating the median value.

Fig. 2 Mean values for net CO_2 assimilation rates (A), stomatal conductance (g_s) and C_i/C_a ± SE for *Populus balsamifera* trees at an atmospheric CO_2 concentration of 400 ppm. The trees were acclimated at either 6 °C (blue solid line) or 10 °C (red dashed line) for six days, and fertilized with high N (HN; panels a, b, c) or low N (LN; panels d, e, f) Hoagland's solution (Table S1 and S2), and measured at leaf temperatures of 2, 6, 10, 14 and 18 °C. A third order polynomial curve was fit for each acclimation temperature for A_{net}, and linear curves were fit for g_s and C_i/C_a.

Fig. 3 Mean values for net CO_2 assimilation rates (A_{net}), stomatal conductance (g_s) and C_i/C_a ± SE for *Populus balsamifera* trees at an atmospheric CO_2 concentration of 2000 ppm. Trees were acclimated at either 6 °C (blue solid line) or 10 °C (red dashed line) for six days, and fertilized

with high N (HN; panels a, b, c) or low N (LN; panels d, e, f) Hoagland's solution (Table S1 and S2), and measured at leaf temperatures of 2, 6, 10, 14 and 18 °C. A third order polynomial curve was fit for each acclimation temperature for A_{net}, and linear curves were fit for stomatal conductance and C_i/C_a.

Fig. 4 Average maximum rates of Rubisco carboxylation (V_{cmax}), electron transport (J_{max}) and dark respiration rates (R_d) ± SE for *Populus balsamifera* trees. The trees were acclimated for six days at 6 °C (solid blue lines) or 10 °C (dashed red lines) and fertilized with high nitrogen (HN; panels a, c, e) or low N (LN; panels b, d, f) Hoagland's solution (Table S1 and S2). The trees were measured at leaf temperatures of 2, 6, 10, 14 and 18 °C, and for each acclimation temperature a third order polynomial curve was fit.

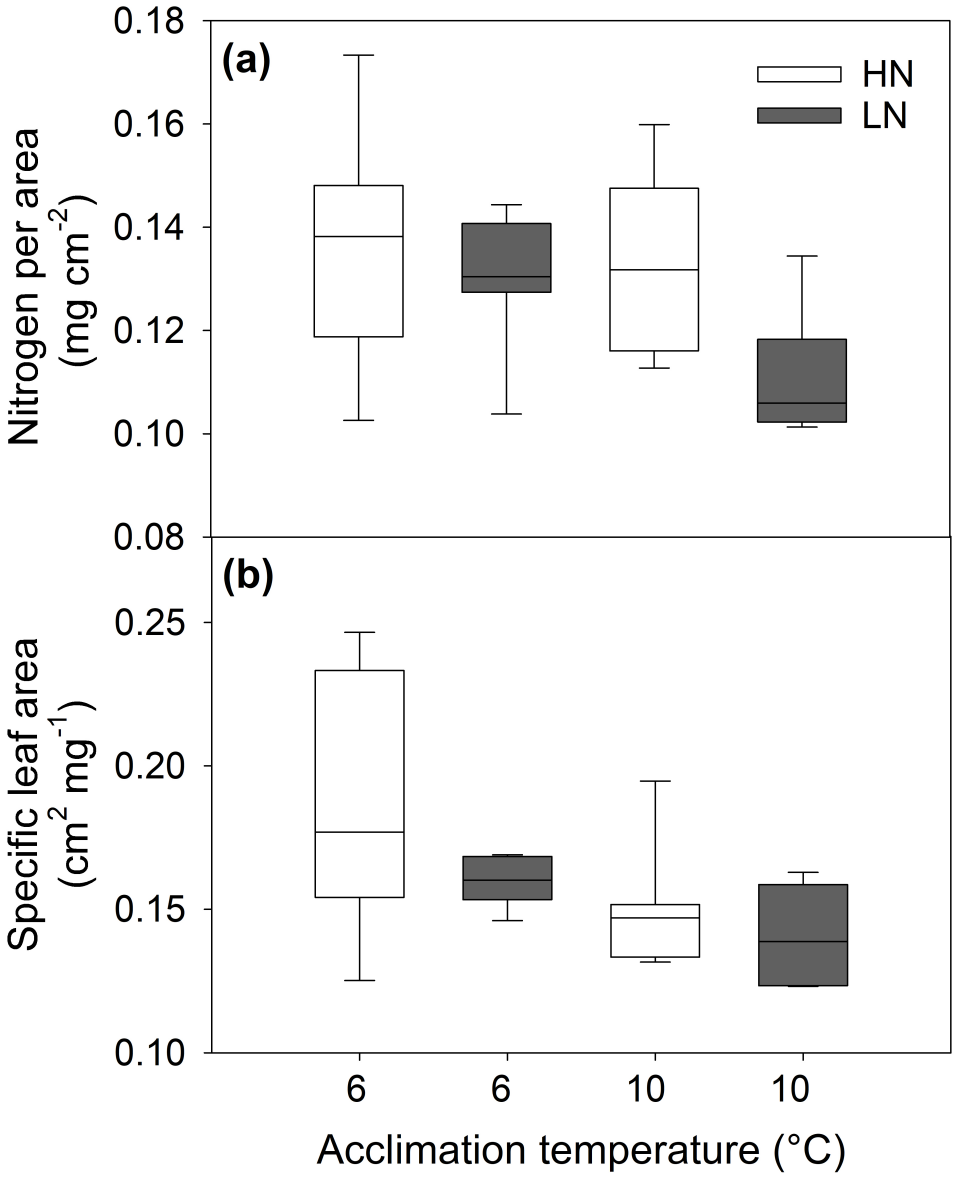
(a)
HN
LN
Nitrogen per area
(mg cm-2)
0.18
0.16
0.14
0.12
0.10
0.08
(b)
Specific leaf area
(cm2 mg-1)
0.25
0.20
0.15
0.10
6
6
10
10
Acclimation temperature (°C)

Fig. 1

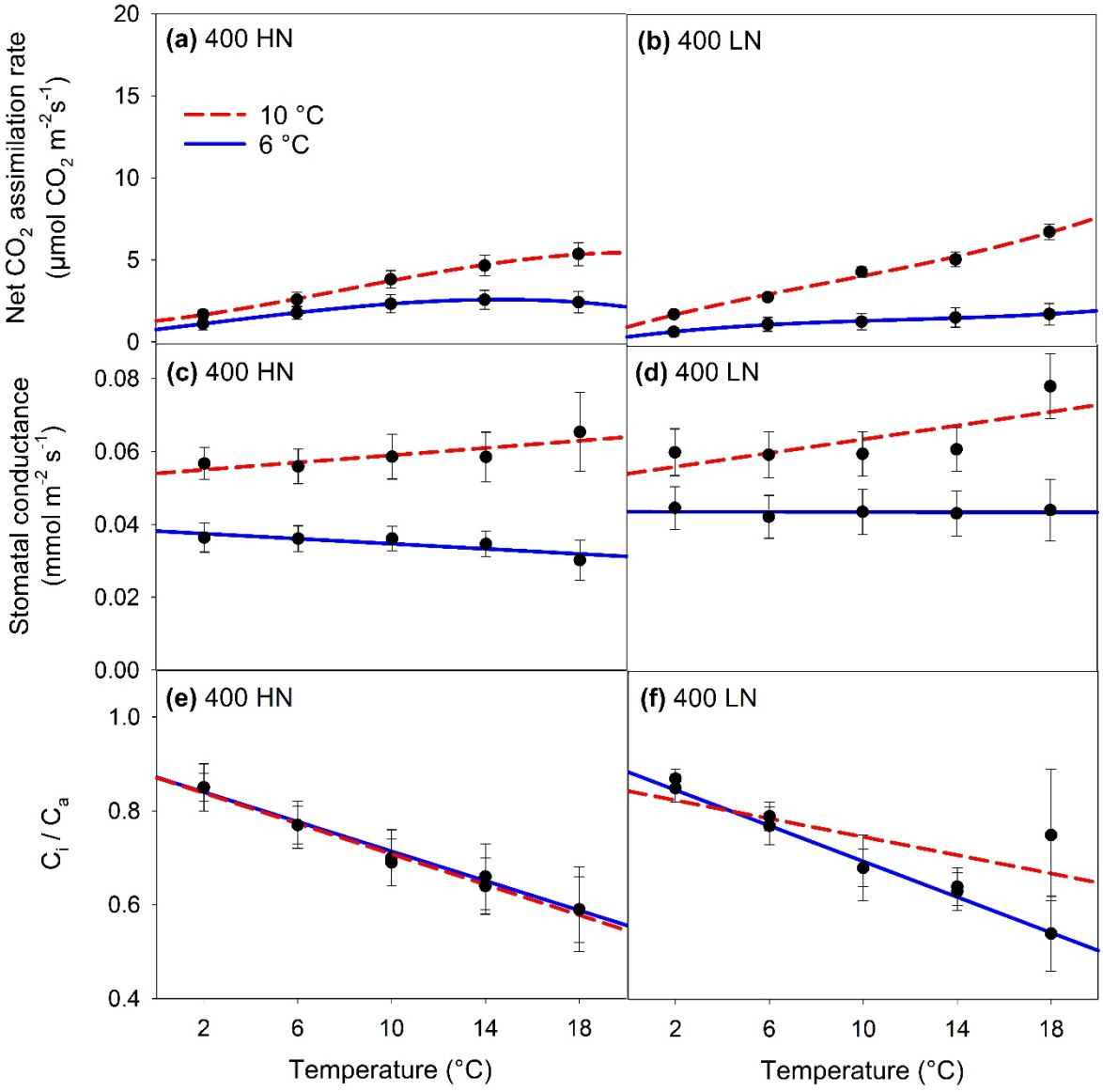
(a) 400 HN
(b) 400 LN
(c) 400 HN
(d) 400 LN
(e) 400 HN
(f) 400 LN
10 °C
6 °C
Net CO2 assimilation rate (μmol CO2 m-2 s-1)
Stomatal conductance (mmol m-2 s-1)
Ci / Ca
Temperature (°C)
Temperature (°C)

Fig. 2

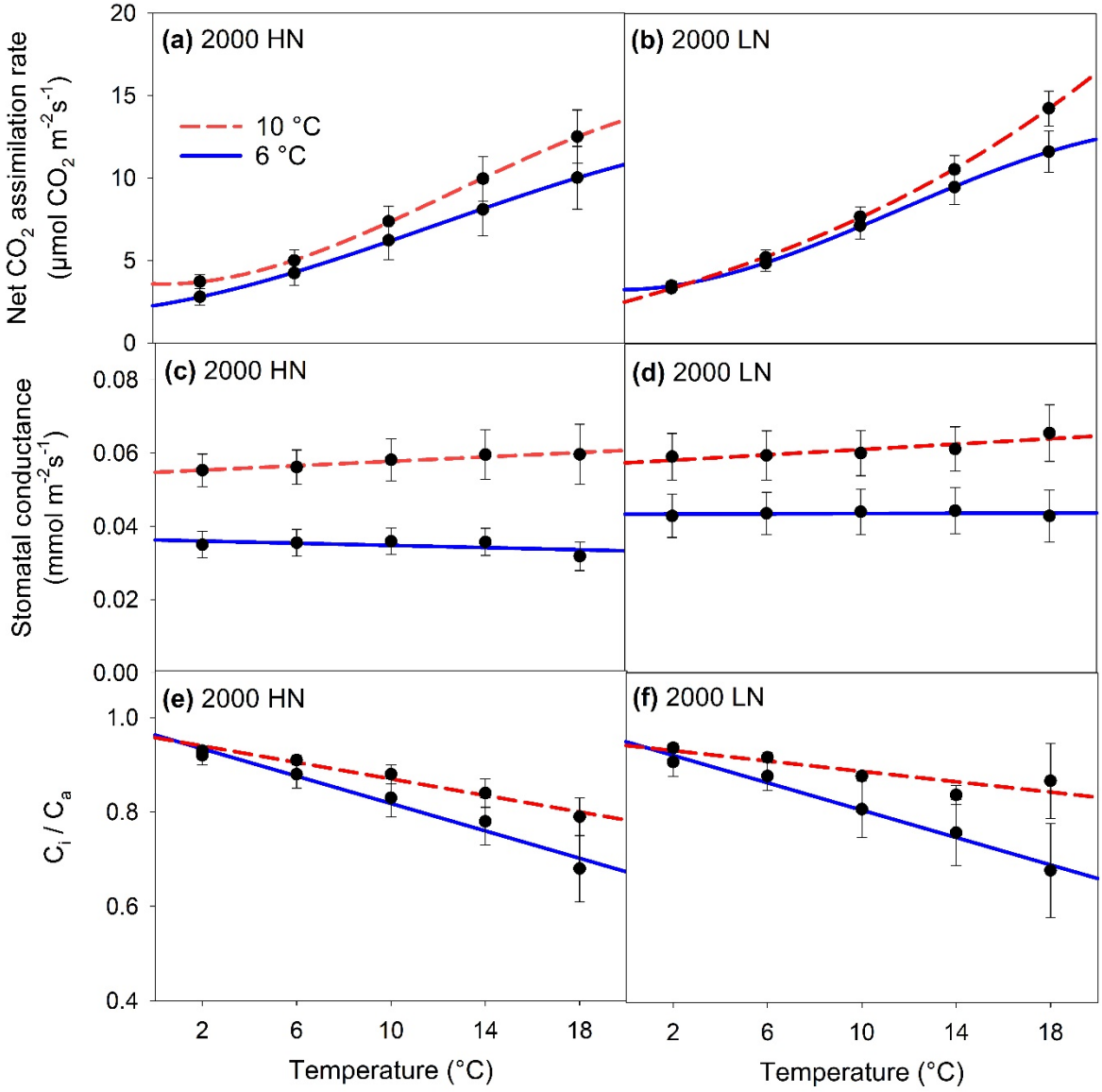
(a) 2000 HN
(b) 2000 LN
(c) 2000 HN
(d) 2000 LN
(e) 2000 HN
(f) 2000 LN
10 °C
6 °C
Net CO2 assimilation rate (μmol CO2 m-2s-1)
Stomatal conductance (mmol m-2s-1)
Ci / Ca
Temperature (°C)
Temperature (°C)

Fig. 3

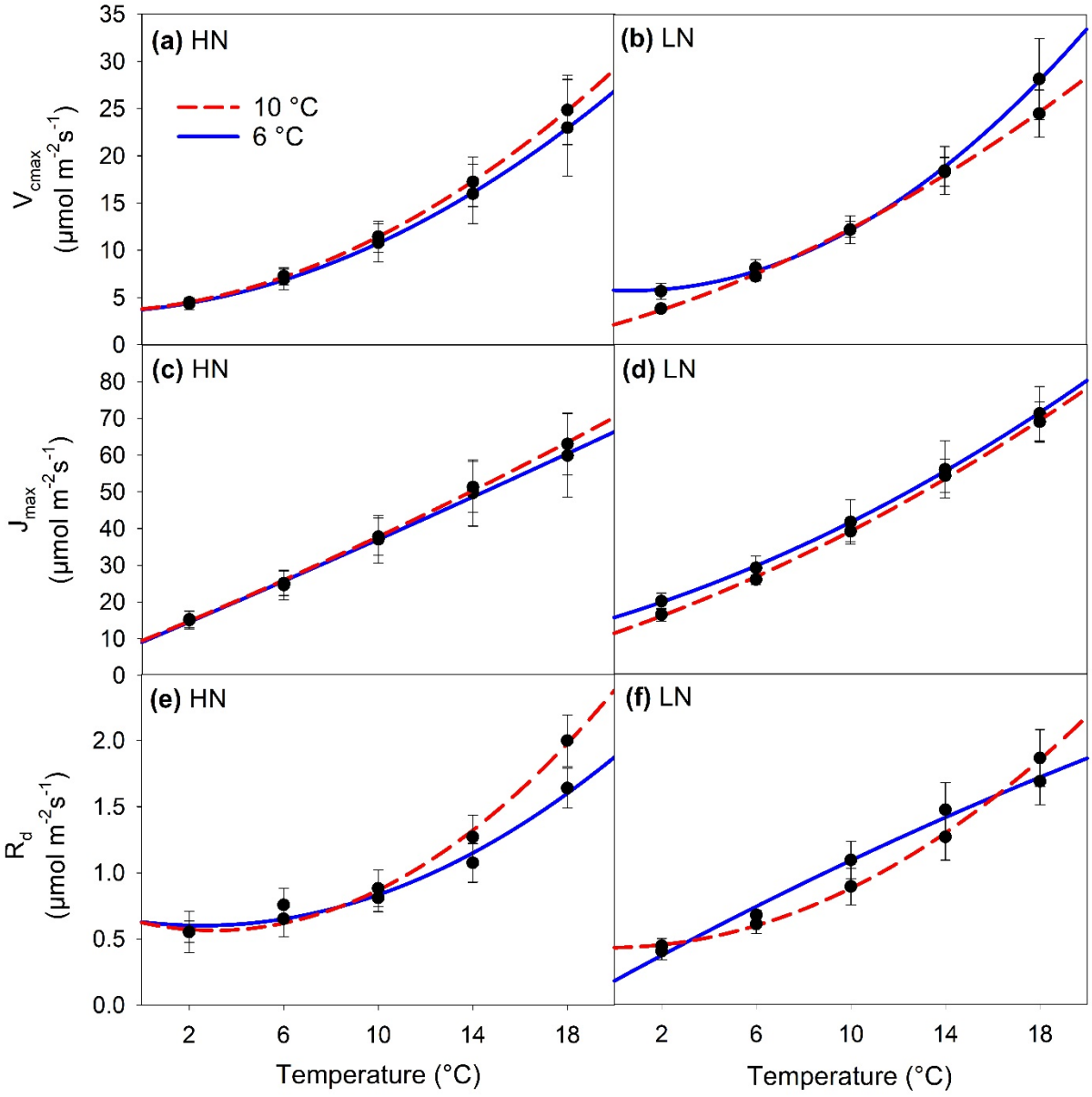
(a) HN
(b) LN
(c) HN
(d) LN
(e) HN
(f) LN
10 °C
6 °C
V_{cmax} (μmol $m^{-2}s^{-1}$)
J_{max} (μmol $m^{-2}s^{-1}$)
R_d (μmol $m^{-2}s^{-1}$)
Temperature (°C)
Temperature (°C)

Fig. 4

Table 1. List of abbreviations with units.

Symbol	Definition	Units
A_{net}	net CO_2 assimilation rate	µmol m^{-2} s^{-1}
$A_{net/DW}$	net CO_2 assimilation rates per unit dry mass	µmol g^{-1} s^{-1}
$A_{net/N}$	net CO_2 assimilation rates per gram nitrogen	µmol g N^{-1} s^{-1}
A_{400}	net CO_2 assimilation rate at an atmospheric CO_2 of 400 ppm	µmol m^{-2} s^{-1}
A_{2000}	net CO_2 assimilation rate at an atmospheric CO_2 of 2000 ppm	µmol m^{-2} s^{-1}
g_s	stomatal conductance	mmol m^{-2} s^{-1}
g_{s400}	stomatal conductance at an atmospheric CO_2 of 400 ppm	mmol m^{-2} s^{-1}
g_{s2000}	stomatal conductance at an atmospheric CO_2 of 2000 ppm	mmol m^{-2} s^{-1}
V_{cmax}	maximal carboxylation rate	µmol m^{-2} s^{-1}
$V_{cmax/DW}$	maximal carboxylation rate per unit dry mass	µmol g^{-1} s^{-1}
$V_{cmax/N}$	maximal carboxylation rate per gram nitrogen	µmol g N^{-1} s^{-1}
J_{max}	maximal electron transport rate	µmol m^{-2} s^{-1}
$J_{max/DW}$	maximal electron transport rate per unit dry mass	µmol g^{-1} s^{-1}
$J_{max/N}$	maximal electron transport rate per gram nitrogen	µmol g N^{-1} s^{-1}
J_{max}/V_{cmax} (JV)	ratio between maximal carboxylation and electron transport rate	
R_d	dark respiration	µmol m^{-2} s^{-1}
$R_{d/DW}$	dark respiration per unit dry mass	µmol g^{-1} s^{-1}
$R_{d/N}$	dark respiration per gram nitrogen	µmol g N^{-1} s^{-1}
T_{leaf}	leaf temperature	°C
$T_{acclimation}$	acclimated temperature leaf	°C
N_{mass}	leaf N concentration	g g^{-1}
N_{area}	leaf N per area basis	mg cm^{-2}
SLA	specific leaf area	cm^2 mg^{-1}
C_i	intercellular CO_2 concentration	µmol m^{-1}
C_a	atmospheric CO_2 concentration	µmol m^{-1}
C_i/C_a	ratio between intercellular and atmospheric CO_2 concentrations	
VPD	vapor pressure deficit	kPa
PAR	photosynthetically active radiation	µmol m^{-2} s^{-1}
k_T	process rate from third-order polynomial equation	µmol m^{-2} s^{-1}
a	exponential coefficient of process rate from third-order polynomial	µmol m^{-2} s^{-1}
b	change in process rate with temperature at 0 °C from third-order polynomial	µmol m^{-2} s^{-1} $°C^{-1}$
c	change in the shape of the curve as temperatures increases from third-order polynomial	µmol m^{-2} s^{-1} $°C^{-2}$

Table 2 Summary statistics for photosynthetic measurements (A_{400}, A_{2000}), stomatal conductance (g_{s400}, g_{s2000}) and the ratio between intercellular and atmospheric CO_2 concentrations (C_i/C_a) for *Populus balsamifera* trees. Measurements were determined at five leaf temperatures (T_{leaf} = 2, 6, 10, 14 and 18 °C) for trees acclimated at one of two temperatures ($T_{acclimation}$ = 6 or 10 °C) under either high nitrogen (HN) or low nitrogen (LN) at an atmospheric CO_2 concentration of 400 or 2000 ppm. Linear mixed models were run with $T_{acclimation}$, T_{leaf} and N level as fixed factors and tree ID as a random factor, and subsequently an ANOVA was performed. The term var. refers to the dependent variable used in the mixed model.

Treatment	**Var.**	***df***	***F***	***P***	**Var.**	***df***	***F***	***P***	**Var.**	***df***	***F***	***P***
$T_{acclimation}$	A_{400}	1,22	10.9	**	g_{s400}	1,22	13.0	**	C_i/C_{a400}	1,24	0.1	
N		1,22	3.1			1,22	1.4			1,52	<0.1	
T_{leaf}		4,88	133.5	**		4,88	3.5	*		4,94	95.7	**
$T_{acclimation} \times$ N		1,22	0.1			1,22	0.1			1,35	<0.1	
$T_{acclimation} \times T_{leaf}$		4,88	19.5	**		4,88	5.7	**		4,94	1.0	
$T_{leaf} \times$ N		4,88	5.6	**		4,88	1.4			4,93	0.5	
$T_{acclimation} \times T_{leaf} \times$ N		4,88	0.1			4,88	0.3			4,93	0.6	
$T_{acclimation}$	A_{2000}	1,23	2.0		g_{s2000}	1,23	12.4	**	C_i/C_{a2000}	1,24	2.8	
N		1,23	1.0			1,23	1.2			1,52	<0.1	
T_{leaf}		4,92	197.6	**		4,92	1.4			4,94	77.2	**
$T_{acclimation} \times$ N		1,23	<0.1			1,23	0.2			1,35	<0.1	
$T_{acclimation} \times T_{leaf}$		4,92	3.0	*		4,92	3.7	**		4,94	2.5	*
$T_{leaf} \times$ N		4,92	1.3			4,92	0.8			4,93	0.8	
$T_{acclimation} \times T_{leaf} \times$ N		4,92	0.2			4,92	0.1			4,93	0.5	

** $P < 0.01$
* $0.01 < P < 0.05$

Table 3 Photosynthetic measurements (A_{400}, A_{2000}, V_{cmax}, J_{max}, and R_d) measured when leaf temperatures (T_{leaf}) is equal to the acclimation temperature ($T_{acclimation}$). Two-way ANOVA models were run with acclimation temperature ($T_{acclimation}$ = 6 °C or 10 °C) and N level (HN – high nitrogen or LN – low nitrogen) as fixed factors; var. refers to the dependent variable used in the ANOVA.

Treatment	**Var.**	***df***	***F***	***P***
$T_{acclimation}$	A_{400}	1, 24	23.3	**
N		1, 24	1.1	
$T_{acclimation} \times N$		1, 24	<0.1	
$T_{acclimation}$	A_{2000}	1, 24	17.8	**
N		1, 24	0.4	
$T_{acclimation} \times N$		1, 24	<0.1	
$T_{acclimation}$	V_{cmax}	1, 24	13.6	**
N		1, 24	0.8	
$T_{acclimation} \times N$		1, 24	< 0.1	
$T_{acclimation}$	J_{max}	1, 24	8.7	**
N		1, 24	0.6	
$T_{acclimation} \times N$		1, 24	0.2	
$T_{acclimation}$	R_d	1, 24	2.1	
N		1, 24	0.1	
$T_{acclimation} \times N$		1, 24	0.1	

** $P < 0.01$
* $0.01 < P < 0.05$

Table 4 Summary statistics for photosynthetic measurements (V_{cmax}, J_{max} and R_d) for *Populus balsamifera* trees. Measurements were determined at five leaf temperatures (T_{leaf} = 2, 6, 10, 14 and 18 °C) for the trees acclimated at one of two temperatures ($T_{acclimation}$ = 6 or 10 °C) under HN – high nitrogen or LN – low nitrogen. Linear mixed models were run with $T_{acclimation}$, T_{leaf} and N level as fixed factors and tree ID as a random factor.

Treatment	**Var.**	***df***	***F***	***P***
$T_{acclimation}$	V_{cmax}	1, 24	<0.1	
N		1, 24	0.5	
T_{leaf}		1, 96	116.7	**
$T_{acclimation} \times N$		1, 24	0.3	
$T_{acclimation} \times T_{leaf}$		4, 96	0.2	
$T_{leaf} \times N$		4, 96	0.3	
$T_{acclimation} \times T_{leaf} \times N$		4. 96	0.4	
$T_{acclimation}$	J_{max}	1, 24	<0.1	
N		1, 24	0.8	
T_{leaf}		1, 96	146.3	**
$T_{acclimation} \times N$		1, 24	0.2	
$T_{acclimation} \times T_{leaf}$		4, 96	0.1	
$T_{leaf} \times N$		4, 96	0.6	
$T_{acclimation} \times T_{leaf} \times N$		4. 96	<0.1	
$T_{acclimation}$	R_d	1, 24	0.1	
N		1, 24	0.1	
T_{leaf}		1, 96	81.8	**
$T_{acclimation} \times N$		1, 24	0.7	
$T_{acclimation} \times T_{leaf}$		4, 96	1.5	
$T_{leaf} \times N$		4, 96	1.4	
$T_{acclimation} \times T_{leaf} \times N$		4, 96	0.7	

** $P < 0.01$
* $0.01 < P < 0.05$

Table 5 Average parameter values from the instantaneous temperature response curves for maximum carboxylation rates (V_{cmax}), maximum electron transport rates (J_{max}) and dark respiration (R_d). Parameters were estimated from Eqn. 1, and two-way ANOVA models were run with acclimation temperature ($T_{acclimation}$ = 6 °C or 10 °C) and N level (HN – high nitrogen or LN – low nitrogen) as fixed factors. For each of the four treatments there were seven replicates, except for the 6 °C – HN treatment, where n = 6.

	Treatment	Mean (SE) a	Mean (SE) b	Mean (SE) c
V_{cmax}	6A HN	3.51 ± 0.58	1.13 ± 0.04	0.9989 ± 0.0016
	6A LN	4.98 ± 0.96	1.10 ± 0.03	1.0004 ± 0.0012
	10A HN	3.51 ± 0.40	1.13 ± 0.02	0.9990 ± 0.0007
	10A LN	2.74 ± 0.30	1.21 ± 0.02	0.9962 ± 0.0006
		F, *P*	*F*, *P*	*F*, *P*
	$T_{acclimation}$	3.35, 0.08	3.62, 0.07	3.38, 0.08
	N	0.32, 0.58	0.55, 0.46	0.30, 0.59
	$T_{acclimation} \times$ N	3.32, 0.08	2.82, 0.11	3.51, 0.07
J_{max}	6A HN	11.71 ± 2.04	1.17 ± 0.05	0.9964 ± 0.0017
	6A LN	17.04 ± 2.79	1.11 ± 0.04	0.9992 ± 0.0017
	10A HN	11.55 ± 1.96	1.17 ± 0.02	0.9968 ± 0.0006
	10A LN	13.12 ± 2.34	1.15 ± 0.03	0.9975 ± 0.0012
		F, *P*	*F*, *P*	*F*, *P*
	$T_{acclimation}$	0.79, 0.38	0.30, 0.59	0.22, 0.64
	N	2.24, 0.15	1.14, 0.30	1.57, 0.22
	$T_{acclimation} \times$ N	0.66, 0.42	0.55, 0.47	0.55, 0.47
R_d	6A HN	0.54 ± 0.09	1.02 ± 0.04	1.0028 ± 0.0018
	6A LN	0.33 ± 0.09	1.22 ± 0.08	0.9954 ± 0.0030
	10A HN	0.57 ± 0.19	1.07 ± 0.08	1.0024 ± 0.0036
	10A LN	0.43 ± 0.10	1.09 ± 0.07	1.0001 ± 0.0033
		F, *P*	*F*, *P*	*F*, *P*
	$T_{acclimation}$	0.25, 0.62	0.35, 0.56	0.71, 0.41
	N	1.93, 0.18	2.31, 0.14	2.07, 0.16
	$T_{acclimation} \times$ N	0.07, 0.80	1.47, 0.24	0.94, 0.34

SUPPLEMENTAL MATERIAL:

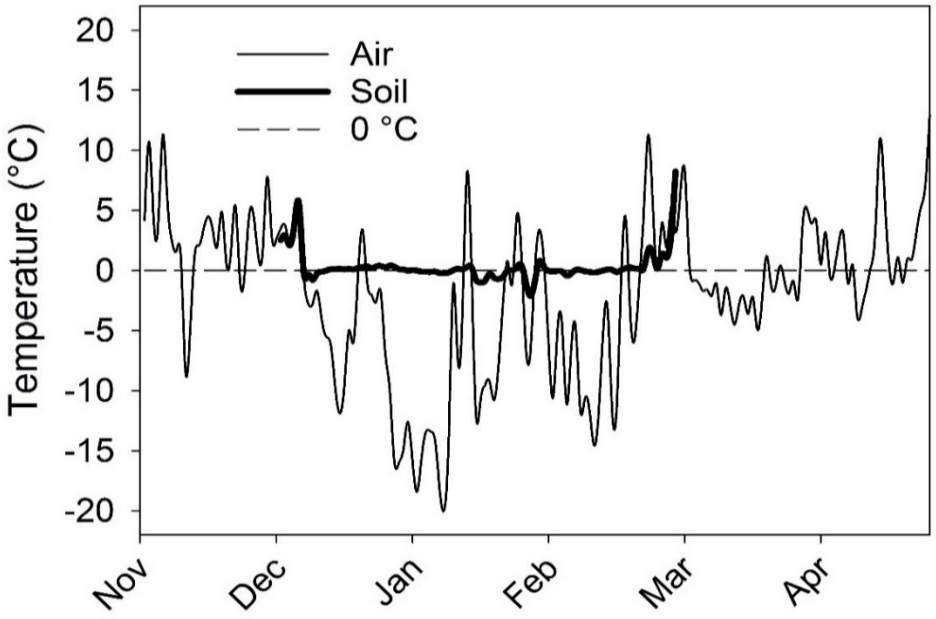

Fig. S1 Average daily air temperatures (non-bold line; Environment Canada, National Climate Data and Information Archive) in London, ON from 16 November 2017 to 23 April 2018 and daily soil surface temperatures (bold line) in the field from 1 December 2017 to 26 February 2018. The trees were brought to the Environmental Sciences Western field station on 16 November 2017 and remained there until 26 February 2018, and temperature loggers were placed on the surface of the pots.

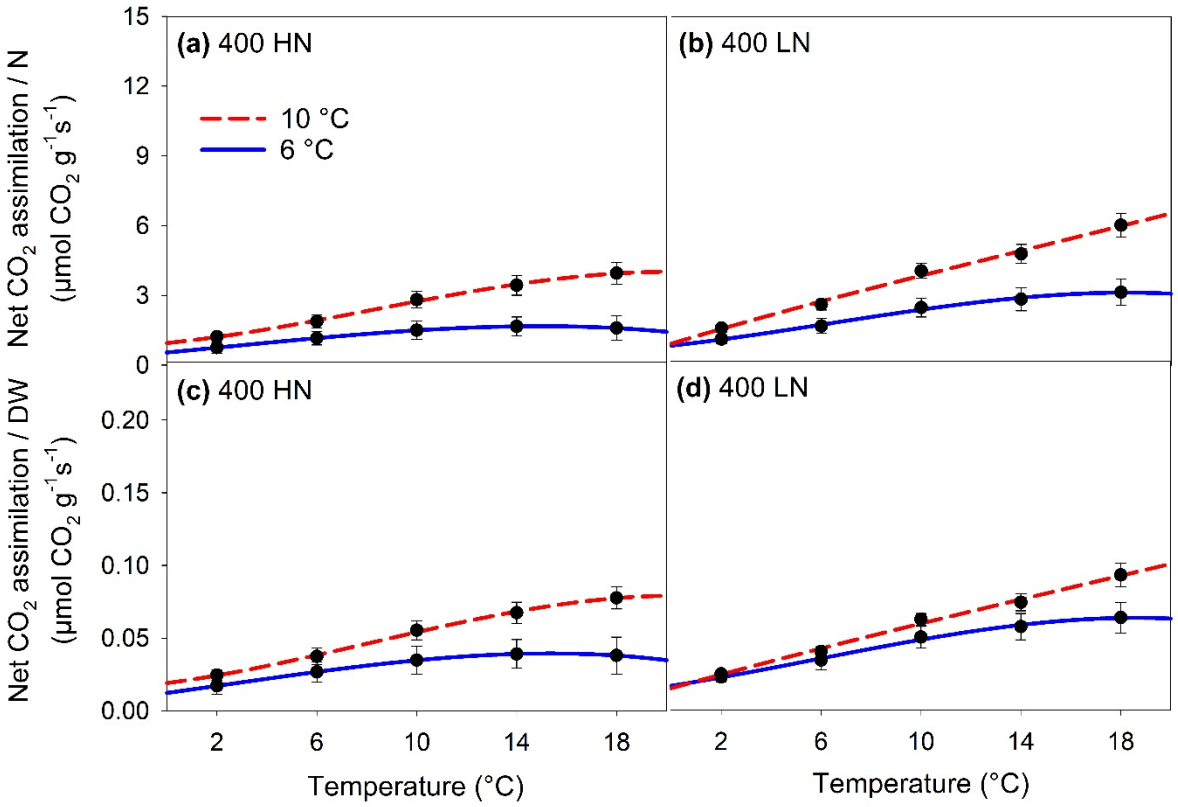

Fig. S2 Mean values for net CO_2 assimilation rates (A_{net}) per nitrogen (N) or per dry weight (DW) ± SE for *Populus balsamifera* trees at an atmospheric CO_2 concentration of 400 ppm. The trees were acclimated at either 6 °C (blue solid line) or 10 °C (red dashed line) for six days, and fertilized with high N (HN; panels a, b, c) or low N (LN; panels d, e, f) Hoagland's solution, and measured at leaf temperatures of 2, 6, 10, 14 and 18 °C. A third order polynomial curve was fit for each acclimation temperature for A_{net}.

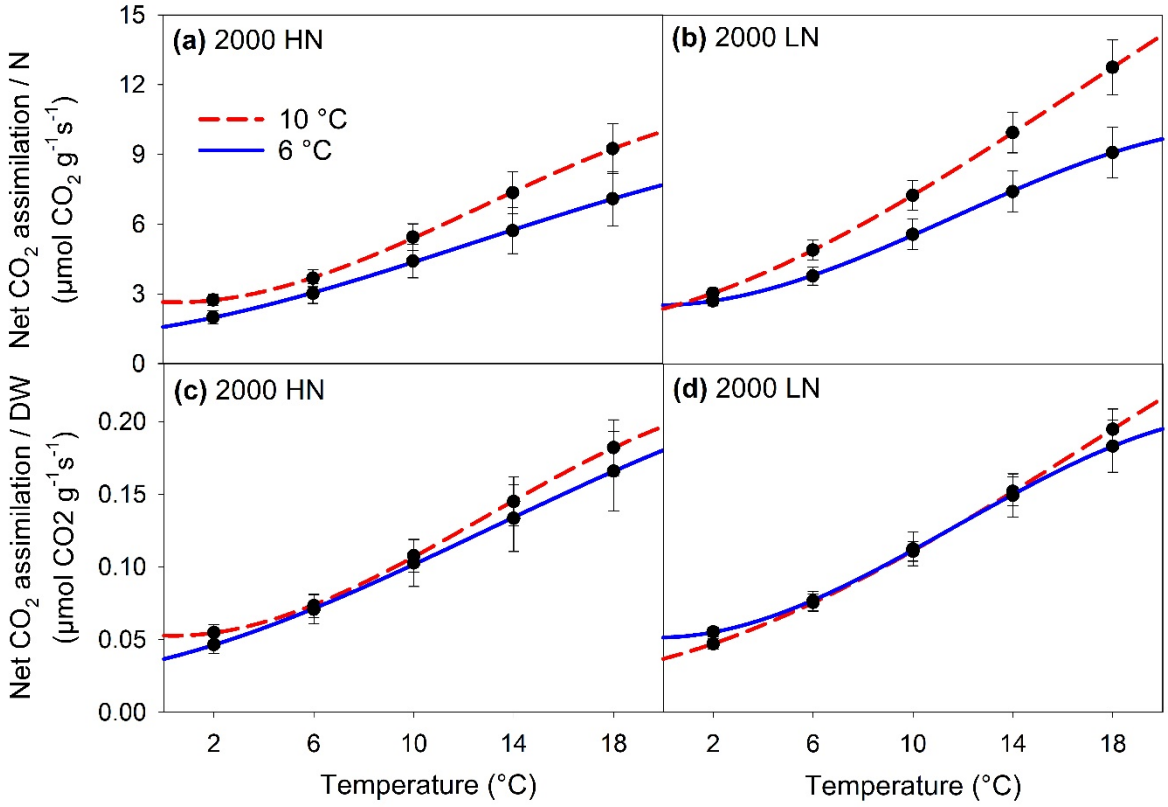

Fig. S3 Mean values for net CO_2 assimilation rates (A_{net}) per nitrogen (N) or per dry weight (DW) ± SE for *Populus balsamifera* trees at an atmospheric CO_2 concentration of 2000 ppm. The trees were acclimated at either 6 °C (blue solid line) or 10 °C (red dashed line) for six days, and fertilized with high N (HN; panels a, b, c) or low N (LN; panels d, e, f) Hoagland's solution, and measured at leaf temperatures of 2, 6, 10, 14 and 18 °C. A third order polynomial curve was fit for each acclimation temperature for A_{net}.

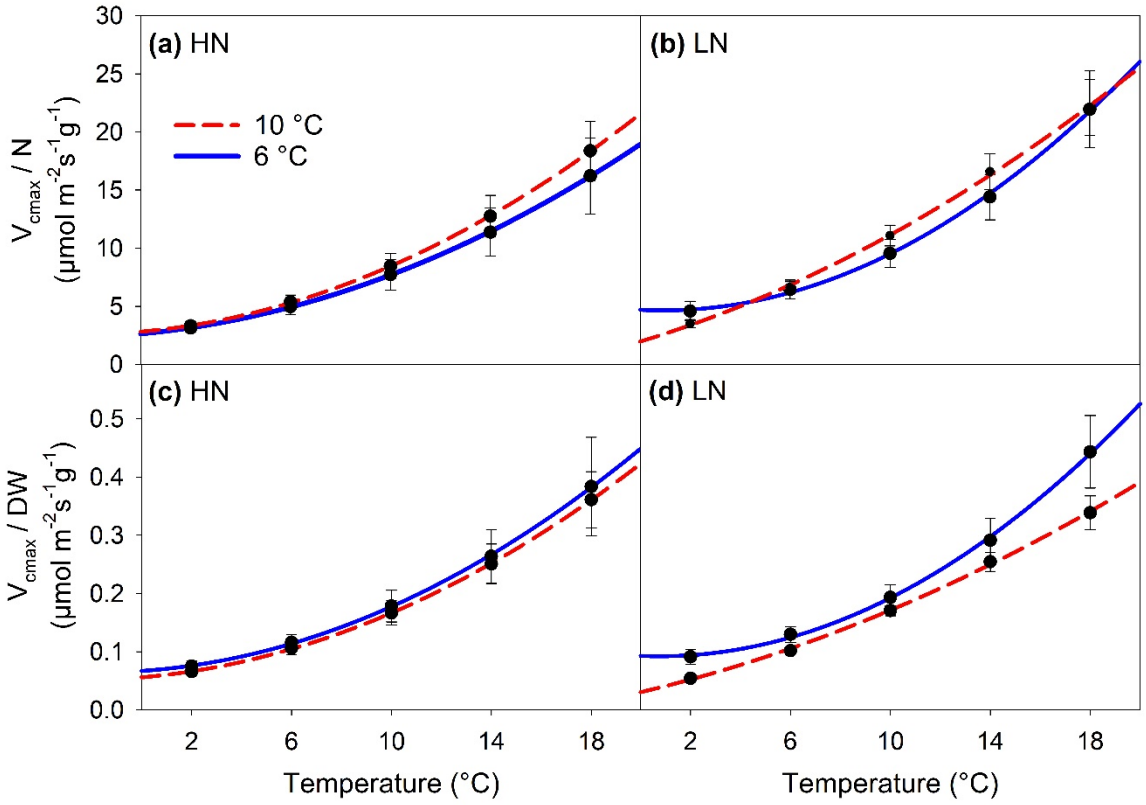

Fig. S4 Average maximum rates of Rubisco carboxylation (V_{cmax}) per nitrogen (N) or per dry weight (DW) ± SE for *Populus balsamifera* trees. The trees were acclimated for six days at 6 °C (solid blue lines) or 10 °C (dashed red lines) and fertilized with high nitrogen (HN; panels a, c, e) or low N (LN; panels b, d, f) Hoagland's solution. The trees were measured at leaf temperatures of 2, 6, 10, 14 and 18 °C, and for each acclimation temperature a third order polynomial curve was fit.

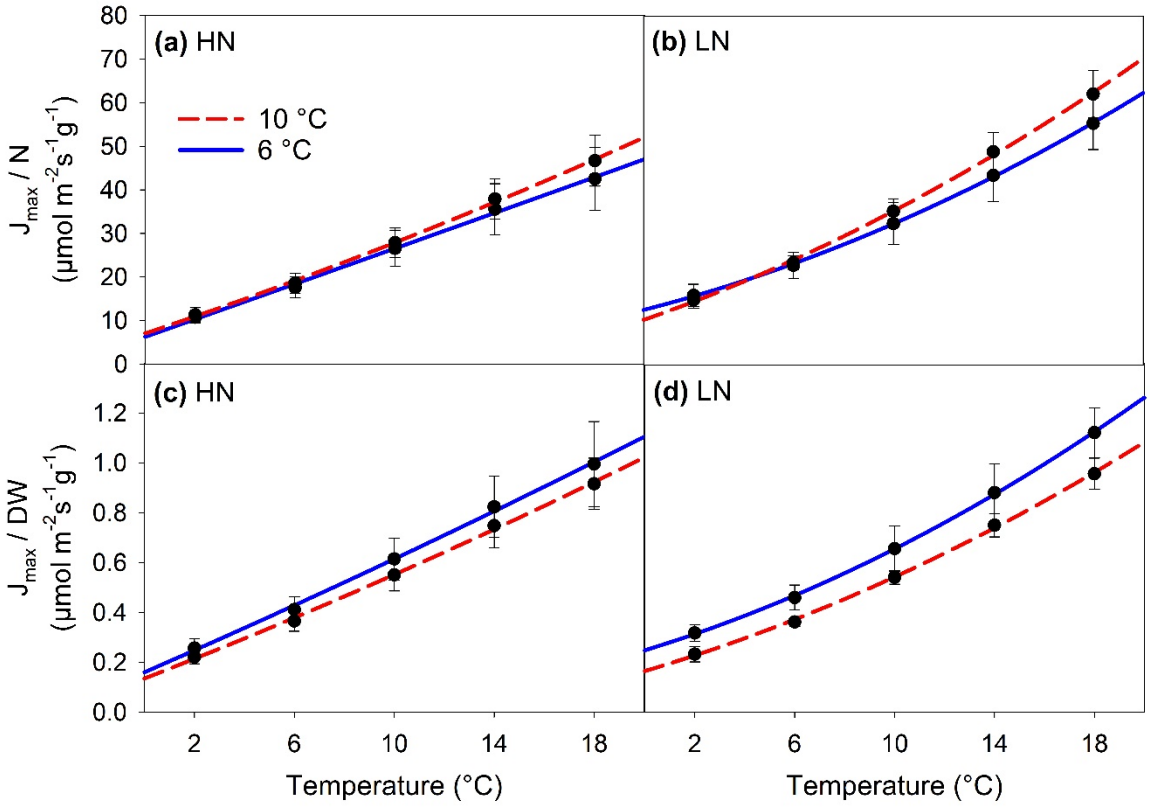

Fig. S5 Average maximum rates of electron transport (J_{max}) per nitrogen (N) or dry weight (DW) ± SE for *Populus balsamifera* trees. The trees were acclimated for six days at 6 °C (solid blue lines) or 10 °C (dashed red lines) and fertilized with high nitrogen (HN; panels a, c, e) or low N (LN; panels b, d, f) Hoagland's solution. The trees were measured at leaf temperatures of 2, 6, 10, 14 and 18 °C, and for each acclimation temperature a third order polynomial curve was fit.

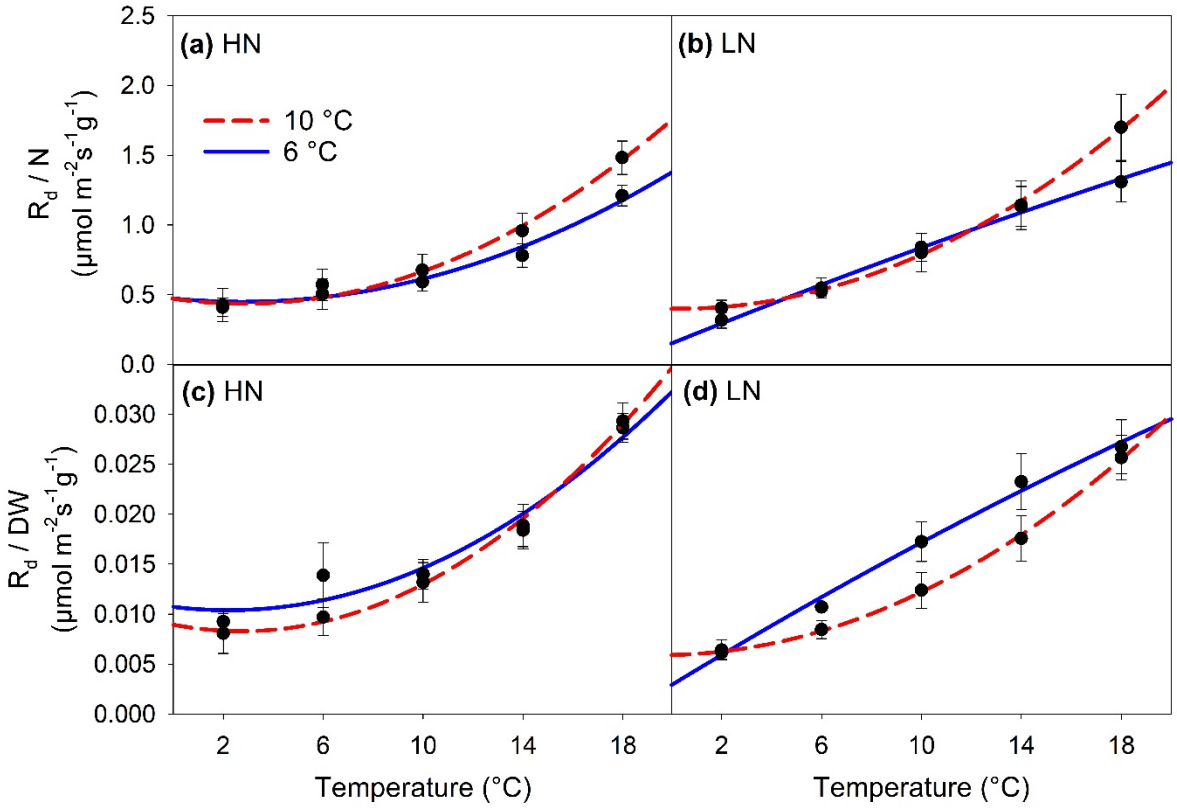

Fig. S6 Average maximum rates of dark respiration (R_d) per nitrogen (N) or per dry weight (DW) ± SE for *Populus balsamifera* trees. The trees were acclimated for six days at 6 °C (solid blue lines) or 10 °C (dashed red lines) and fertilized with high nitrogen (HN; panels a, c, e) or low N (LN; panels b, d, f) Hoagland's solution. The trees were measured at leaf temperatures of 2, 6, 10, 14 and 18 °C, and for each acclimation temperature a third order polynomial curve was fit.

Table S1 Molarity and quantity of stock solutions required for the half strength Hoagland's solution.

Compound	**Molarity (M)**	**Amount (mL)**
K_2SO_4	0.5	10
$CaCl_2 – 2H_2O$	1.0	10
KH_2PO_4	1.0	5
$MgSO_4 – 8H_2O$	1.0	2.5
Fe-EDTA	0.02	2.5
NH_4NO_3	1.0	40 (HN) or 0 (LN)
Micronutrients	Variable	2.5

Table S2 Molarity of chemical compounds in the micronutrient stock solution.

Compound	Molarity (M)
BH_3O_3	0.05
$MNSO_4 \cdot H_2O$	0.01
$ZnSO_4$	0.001
$CuSO_4$	0.0005
$Na_2MoO_4 \cdot 2H_2O$	0.0005

Table S3 Nitrogen expressed on a per mass (N_{mass}) and per area (N_{area}) basis, and specific leaf area (SLA) values for *Populus balsamifera* leaves acclimated at 6 or 10 °C ($T_{acclimation}$) with two N levels (N) of high (HN) or low nitrogen (LN) fertilizer for six days. Var. refers to the dependent variable of interest.

Var.	**Treatment**	***df***	***F***	***P***
N_{mass}	$T_{acclimation}$	1, 24	15.7	<0.01**
	N	1, 24	11.0	<0.01**
	$T_{acclimation} \times N$	1, 24	0.3	0.62
N_{area}	$T_{acclimation}$	1, 24	2.4	0.14
	N	1, 24	4.3	0.05*
	$T_{acclimation} \times N$	1, 24	1.9	0.18
SLA	$T_{acclimation}$	1, 24	6.5	0.02*
	N	1, 24	2.9	0.10
	$T_{acclimation} \times N$	1, 24	0.4	0.52

** $P < 0.01$
* $0.01 < P < 0.05$

Table S4 Summary statistics for photosynthetic measurements (A_{400}, A_{2000}) per nitrogen (N) and dry weight (DW) for *Populus balsamifera* trees at an atmospheric CO_2 concentration of 400 or 2000 ppm. Measurements were determined at five leaf temperatures (T_{leaf}; 2, 6, 10, 14 and 18 °C) for the trees acclimated at 6 or 10 °C ($T_{acclimation}$) for six days under two N levels (N; HN – high nitrogen or LN – low nitrogen). Linear mixed models were run with acclimation temperature, leaf temperature and N level as fixed factors and tree ID as a random factor. Var. refers to the dependent variable including A_{net} at an atmospheric CO_2 concentration of 400 ppm expressed on a per nitrogen ($A_{400/N}$) and dry weight ($A_{400/DW}$) basis, and A_{net} at an atmospheric CO_2 concentration of 2000 ppm expressed on a per nitrogen ($A_{2000/N}$) and dry weight ($A_{2000/DW}$) basis.

Treatment	**Var.**	***df***	***F***	***P***	**Var.**	***df***	***F***	***P***
$T_{acclimation}$	$A_{400/N}$	1,22	17.2	<0.01**	$A_{400/DW}$	1,22	6.6	0.02*
N		1,22	9.0	†<0.01**		1,22	2.4	0.13
T_{leaf}		4,88	132.5	<0.01**		4,88	136.4	<0.01**
$T_{acclimation} \times N$		1,22	0.1	0.74		1,22	0.4	0.56
$T_{acclimation} \times T_{leaf}$		4,88	23.3	<0.01**		4,88	13.8	<0.01**
$T_{leaf} \times N$		4,88	10.2	<0.01**		4,88	4.6	<0.01**
$T_{acclimation} \times T_{leaf} \times N$		4,88	0.3	0.89		4,88	0.2	0.92
$T_{acclimation}$	$A_{2000/N}$	1,23	5.5	†0.03*	$A_{2000/DW}$	1,23	0.2	0.70
N		1,23	5.6	†0.03*		1,23	0.4	0.54
T_{leaf}		4,92	209.6	<0.01**		4,92	226.4	<0.01**
$T_{acclimation} \times N$		1,23	0.2	0.64		1,23	0.1	0.75
$T_{acclimation} \times T_{leaf}$		4,92	6.1	<0.01**		4,92	0.7	‡0.61
$T_{leaf} \times N$		4,92	5.3	†<0.01**		4,92	0.7	0.61
$T_{acclimation} \times T_{leaf} \times N$		4,92	0.9	0.50		4,92	0.1	0.97

** $P < 0.01$
* $0.01 < P < 0.05$
† Difference in significance between per area and per N measurements
‡ Difference in significance between per area and per DW measurements

Table S5 Photosynthetic measurements (A_{400}, A_{2000}, V_{cmax}, J_{max}, and R_d) per nitrogen (N) and dry weight (DW) measured when $T_{leaf} = T_{acclimation}$. Two-way ANOVA models were run with acclimation temperature ($T_{acclimation}$; 6 °C or 10 °C) and N level (N; HN – high nitrogen or LN – low nitrogen) as fixed factors. The dependent variables (Var.) include carbon assimilation rates at atmospheric CO_2 concentrations of 400 or 2000 ppm on a per nitrogen ($A_{400/N}$) and dry weight ($A_{400/DW}$) basis, maximum carboxylation rates on a per nitrogen ($V_{cmax/N}$) and dry weight ($V_{cmax/DW}$) basis, maximum electron transport rates on a per nitrogen ($J_{max/N}$) and dry weight ($J_{max/DW}$) basis, and dark respiration rates on a per nitrogen ($R_{d/N}$) and dry weight ($R_{d/DW}$) basis.

Treatment	**Var.**	***df***	***F***	***P***	**Var.**	***df***	***F***	***P***
$T_{acclimation}$	$A_{400/N}$	1, 24	35.1	<0.01**	$A_{400/DW}$	1, 24	19.2	<0.01**
N		1, 24	5.8	†0.02*		1, 24	0.7	0.41
$T_{acclimation} \times$ N		1, 24	0.9	0.34		1, 24	<0.1	0.96
$T_{acclimation}$	$A_{2000/N}$	1, 24	29.2	<0.01**	$A_{2000/DW}$	1, 24	14.2	<0.01**
N		1, 24	4.7	†0.04*		1, 24	0.1	0.79
$T_{acclimation} \times$ N		1, 24	0.5	0.49		1, 24	0.2	0.70
$T_{acclimation}$	$V_{cmax/N}$	1, 24	24.0	<0.01**	$V_{cmax/DW}$	1, 24	9.4	<0.01**
N		1, 24	6.0	†0.02*		1, 24	0.3	0.56
$T_{acclimation} \times$ N		1, 24	1.2	0.28		1, 24	0.1	0.75
$T_{acclimation}$	$J_{max/N}$	1, 24	17.3	<0.01**	$J_{max/DW}$	1, 24	4.8	0.04*
N		1, 24	5.4	†0.03*		1, 24	0.1	0.70
$T_{acclimation} \times$ N		1, 24	0.6	0.46		1, 24	0.3	0.57
$T_{acclimation}$	$R_{d/N}$	1, 24	3.3	0.08	$R_{d/DW}$	1, 24	0.5	0.83
N		1, 24	0.1	0.71		1, 24	0.6	0.46
$T_{acclimation} \times$ N		1, 24	0.7	0.42		1, 24	0.2	0.66

** $P < 0.01$
* $0.01 < P < 0.05$
† Difference in significance between per area and per N measurements

Table S6 Summary statistics for photosynthetic measurements (V_{cmax}, J_{max} and R_d) on a nitrogen (N) or dry weight (DW) basis for *Populus balsamifera* trees. Measurements were determined at five leaf temperatures (2, 6, 10, 14 and 18 °C) for the trees acclimated at 6 or 10 °C for six days under HN – high nitrogen or LN – low nitrogen. Linear mixed models were run with acclimation temperature ($T_{acclimation}$), leaf temperature (T_{leaf}) and N level (N) as fixed factors and tree ID as a random factor. The dependent variables (Var.) include maximum carboxylation rates on a per nitrogen ($V_{cmax/N}$) and dry weight ($V_{cmax/DW}$) basis, maximum electron transport rates on a per nitrogen ($J_{max/N}$) and dry weight ($J_{max/DW}$) basis, and dark respiration rates on a per nitrogen ($R_{d/N}$) and dry weight ($R_{d/DW}$) basis.

Treatment	**Var.**	***df***	***F***	***P***	**Var.**	***df***	***F***	***P***
$T_{acclimation}$	$V_{cmax/N}$	1, 24	0.3	0.56	$V_{cmax/DW}$	1, 24	1.3	0.26
N		1, 24	3.5	0.07		1, 24	0.2	0.70
T_{leaf}		4, 96	133.3	<0.01**		1, 96	116.4	<0.01**
$T_{acclimation} \times N$		1, 24	<0.1	0.89		1, 24	0.4	0.53
$T_{acclimation} \times T_{leaf}$		4, 96	0.6	0.66		4, 96	0.7	0.59
$T_{leaf} \times N$		4, 96	2.0	0.10		4, 96	0.1	0.99
$T_{acclimation} \times T_{leaf} \times N$		4. 96	0.3	0.87		4. 96	0.4	0.82
$T_{acclimation}$	$J_{max/N}$	1, 24	0.4	0.52	$J_{max/DW}$	1, 24	1.8	0.19
N		1, 24	4.7	†0.03*		1, 24	0.3	0.58
T_{leaf}		4, 96	163.0	<0.01**		1, 96	161.2	<0.01**
$T_{acclimation} \times N$		1, 24	<0.1	0.89		1, 24	0.2	0.66
$T_{acclimation} \times T_{leaf}$		4, 96	0.9	0.47		4, 96	0.3	0.90
$T_{leaf} \times N$		4, 96	2.7	†0.03*		4, 96	0.3	0.86
$T_{acclimation} \times T_{leaf} \times N$		4. 96	0.2	0.95		4. 96	<0.1	0.99
$T_{acclimation}$	$R_{d/N}$	1, 24	1.4	0.25	$R_{d/DW}$	1, 24	2.7	0.11
N		1, 24	1.9	0.18		1, 24	0.6	0.46
T_{leaf}		4, 96	79.3	<0.01**		1, 96	85.9	<0.01**
$T_{acclimation} \times N$		1, 24	<0.1	0.99		1, 24	0.6	0.45
$T_{acclimation} \times T_{leaf}$		4, 96	2.3	0.07		4, 96	0.6	0.65
$T_{leaf} \times N$		4, 96	2.1	0.09		4, 96	1.7	0.17
$T_{acclimation} \times T_{leaf} \times N$		4. 96	0.5	0.72		4. 96	1.0	0.41

** $P < 0.01$
* $0.01 < P < 0.05$
† Difference in significance between per area and per N measurements

Table S7 Summary statistics for the ratio of J_{max}/V_{cmax} (JV) *Populus balsamifera* trees acclimated at 6 or 10 °C for six days under HN – high nitrogen or LN – low nitrogen. Measurements were determined at five leaf temperatures (2, 6, 10, 14 and 18 °C), and linear mixed models were run with acclimation temperature ($T_{acclimation}$), leaf temperature (T_{leaf}) and N level (N) as fixed factors and tree ID as a random factor.

Treatment	***df***	***F***	***P***
$T_{acclimation}$	1, 24	<0.1	0.90
N	1, 24	0.7	0.42
T_{leaf}	4, 96	13.8	<0.01**
$T_{acclimation} \times$ N	1, 24	1.6	0.22
$T_{acclimation} \times T_{leaf}$	4, 96	0.7	0.58
$T_{leaf} \times$ N	4, 96	2.3	0.06
$T_{acclimation} \times T_{leaf} \times$ N	4. 96	0.3	0.88

** $P < 0.01$
* $0.01 < P < 0.05$

Table S8 Mean ratios of J/V ± SE for *Populus balsamifera* trees acclimated at 6 or 10 °C ($T_{acclimation}$; 6A and 10A, respectively) with two N levels (N; high (HN) or low nitrogen (LN)) fertilizer. J_{max} and V_{cmax} were determined using temperature response curves when leaf temperature was equal to the acclimation temperature ($T_{leaf} = T_{acclimation}$).

Treatment	**J_{max}/V_{cmax} ± SE**
6A HN	3.53 ± 0.13
6A LN	3.54 ± 0.13
10A HN	3.35 ± 0.07
10A LN	3.18 ± 0.04
	F, *P*
$T_{acclimation}$	7.3, 0.01 *
N	0.6, 0.43
$T_{acclimation} \times N$	0.7, 0.40

** $P < 0.01$
* $0.01 < P < 0.05$